EUROPEAN RESPIRATORY journal
FLAGSHIP SCIENTIFIC JOURNAL OF ERS

Early View

Original article

6-mercaptopurine, an agonist of Nur77, reduces progression of pulmonary hypertension by enhancing BMP signalling

Kondababu Kurakula, Xiao-Qing Sun, Chris Happé, Denielli da Silva Goncalves Bos, Robert Szulcek, Ingrid Schalij, Karien C. Wiesmeijer, Kirsten Lodder, Ly Tu, Christophe Guignabert, Carlie J. M. de Vries, Frances S. de Man, Anton Vonk Noordegraaf, Peter ten Dijke, Marie-José Goumans, Harm Jan Bogaard

Please cite this article as: Kurakula K, Sun X-Q, Happé C, *et al*. 6-mercaptopurine, an agonist of Nur77, reduces progression of pulmonary hypertension by enhancing BMP signalling. *Eur Respir J* 2019; in press (https://doi.org/10.1183/13993003.02400-2018).

6-mercaptopurine, an agonist of Nur77, reduces progression of pulmonary hypertension by enhancing BMP signalling

Kondababu Kurakula[1,7], Xiao-Qing Sun[2,7], Chris Happé[2], Denielli da Silva Goncalves Bos[2], Robert Szulcek[2], Ingrid Schalij[2], Karien C. Wiesmeijer[1], Kirsten Lodder[1], Ly Tu[3,4], Christophe Guignabert[3,4], Carlie J.M. de Vries[5], Frances S. de Man[2], Anton Vonk Noordegraaf[2], Peter ten Dijke[6], Marie-José Goumans[1,8], Harm Jan Bogaard[2,8]

[1]Department of Cell and Chemical Biology, Leiden University Medical Center, Leiden, The Netherlands. [2]Pulmonary Hypertension Knowledge Center, Department of Pulmonology, VU University Medical Center/Institute for Cardiovascular Research, Amsterdam, The Netherlands. [3]INSERM UMR_S 999, LabEx LERMIT, Hôpital Marie Lannelongue, Le Plessis-Robinson, France. [4]Université Paris-Sud et Université Paris-Saclay, Le Kremlin-Bicêtre, France. [5]Department of Medical Biochemistry, Academic Medical Center, Amsterdam, The Netherlands. [6]Department of Cell and Chemical Biology, Oncode institute, Leiden University Medical Center, Leiden, The Netherlands. [7]These two authors contributed equally to this work.[8]These two authors jointly supervised this work.

Corresponding authors

Harm Jan Bogaard, MD PhD
Amsterdam UMC
Vrije Universiteit Amsterdam
Department of Pulmonary Medicine
Amsterdam Cardiovascular Sciences
de Boelelaan 1117
Amsterdam, the Netherlands
Tel: +31 20 44 4328
Fax: +31 20 44 4328
Email: HJ.Bogaard@vumc.nl

Marie-José Goumans
Leiden University Medical Center
Dept Cell and Chemical Biology
Laboratory for Cardiovascular Cell Biology
Email: M.J.T.H.Goumans@lumc.nl

Take home message

Pharmacological activation of Nur77 with 6-mercaptopurine reduces the progression of pulmonary hypertension by enhancing BMP signalling

Abstract:
Pulmonary arterial hypertension (PAH) is a progressive fatal disease characterized by abnormal remodelling of pulmonary vessels, leading to increased vascular resistance and right ventricle failure. This abnormal vascular remodelling is associated with endothelial cell dysfunction, increased proliferation of smooth muscle cells, inflammation, and impaired bone morphogenetic protein (BMP) signalling. Orphan nuclear receptor Nur77 is a key regulator of proliferation and inflammation in vascular cells, but its role in the impaired BMP signaling and vascular remodelling in PAH is unknown.

We hypothesized that activation of Nur77 by 6-mercaptopurine would improve the PAH by inhibiting endothelial cell dysfunction and vascular remodelling.

Nur77 expression is decreased in cultured pulmonary microvascular endothelial cells (MVECs) and lungs of PAH patients. Nur77 significantly increased BMP signaling and strongly decreased proliferation and inflammation in MVECs. In addition, conditioned medium from PAH MVECs overexpressing Nur77 inhibited the growth of healthy smooth muscle cells. Pharmacological activation of Nur77 by 6-mercaptopurine markedly restored MVEC function by normalizing proliferation, inflammation and BMP signaling. Finally, 6-mercaptopurine prevented and reversed abnormal vascular remodelling and right ventricle hypertrophy in the sugen-hypoxia rat model of severe angioproliferative PAH.

Our data demonstrate that Nur77 is a critical modulator in PAH by inhibiting vascular remodelling and increasing BMP signalling, and activation of Nur77 could be a promising option for the treatment of PAH.

Introduction

Pulmonary arterial hypertension (PAH) is a progressive fatal disease caused by abnormal proliferation of pulmonary vascular cells, resulting in remodelling of small pulmonary arteries (PAs), increased pulmonary vascular resistance, right ventricular (RV) failure, and ultimately death [1-4]. In hereditary PAH, mutations in the gene encoding for bone morphogenetic protein receptor 2 (BMPR2) or in genes encoding for downstream SMAD transcriptional effectors lead to impaired BMP signaling [4-7]. Interestingly, Impaired BMP signalling also occurs in non-hereditary forms of PAH [6, 8]. Despite advances in the treatment of PAH, current therapies still fail to reverse the established abnormal remodelling present in the lungs. Therefore, new molecular targets for development of remodelling-focused therapeutics are urgently needed.

Pulmonary artery endothelial cells (PA-ECs), pulmonary artery smooth muscle cells (PA-SMCs), pericytes and fibroblasts all play crucial roles in the pathobiology of PAH [5, 9-12]. PAH PA-ECs are hyperproliferative and contribute to the decrease in luminal diameter of the pulmonary micro-vessels. Additionally, PAH PA-ECs secrete factors such as inflammatory cytokines and growth factors which in turn induce proliferation and migration of PA-SMCs and fibroblasts and contribute to the progression of PAH [13-17]. A loss of BMPR2 in the endothelium can initiate and sustain the development of PAH [18, 19], but the driving transcriptional mechanisms remain poorly understood. Here we identify a central role for the orphan nuclear receptor Nur77 (NR4A1) in EC dysfunction, aberrant BMP signalling and vascular remodelling in PAH.

The transcription factor Nur77 plays a key role in a wide array of cellular processes such as proliferation, apoptosis, and inflammation [20-25]. Nur77 is implicated in several cardiovascular diseases such as atherosclerosis, restenosis, and cardiac hypertrophy [20, 22, 26]. In ECs, Nur77 decreases endothelin-1 expression and attenuates pro-inflammatory responses via inhibition of the nuclear factor (NF)κB pathway [27, 28]. Activation of Nur77 by Cytosporone B (CsnB) was shown to ameliorate experimental pulmonary hypertension (PH) in mice by decreasing PA-SMC proliferation [25, 29]. Interestingly, Nur77 modulates the transforming growth factor β (TGFβ) pathway in a cell-and context- dependent manner [30, 31]. 6-Mercaptopurine (6-MP), a well-established immunosuppressive drug to treat various autoimmune and chronic inflammatory diseases, is a non-traditional agonist of Nur77 [21, 22, 32]. 6-MP mediates a genotoxic stress response which in turn activates transcription of all three members of the NR4A nuclear hormone receptor family, including Nur77, NOR-1, and Nurr1 [32]. We and others have shown that 6-MP inhibits activation of immune cells and also reduces the inflammatory response of ECs and the proliferation of vascular SMCs in a Nur77 dependent manner [33-35]. Here, we show that Nur77 is a key player in PAH, involved in PA-EC dysfunction, proliferation of PA-SMCs and impaired BMP signalling, and that pharmacological targeting of Nur77 by 6-MP presents a novel therapeutic concept in PAH.

Methods

See supplementary material for detailed methods.

Human lung samples and cell culture

PAH lung tissues were collected with patients' consent and approval from the local ethics committees at Free medical center, Amsterdam and Comite de ´Protection des Personnes (CPP) Ile-de-France VII, Paris. Control lung tissue was from patients undergoing a surgical procedure for cancer. Isolation and culturing of microvascular endothelial cells (MVECs) and pulmonary artery smooth muscle cells (PA-SMCs) was described previously [36, 37].

Plasmids, chemicals, Quantitative Real Time-PCR (qRT-PCR), western blot and luciferase assays

See supplementary material for details.

Lenti-viral transduction and proliferation assays
Lenti-viral transduction of cells, and cell proliferation (MTT) assays were performed as described previously [21, 23].

SuHx rat model of pulmonary hypertension (PH)
SU5416+Hypoxia (SuHx)-mediated PH in male Sprague-Dawley rats was induced as described previously [38, 39]. In the prevention study, rats received 6-MP (1 mg/kg/day) in drinking water from day 0 to day 42. In the reversal study, after randomization (treatment vs vehicle), animals were divided into two groups receiving 6-MP (1 mg/kg/day or 7.5 mg/kg/day) or vehicle (DMSO) in the drinking water from day 42 to day 70. Power calculation was performed to determine the appropriate sample size for both prevention and reversal studies. Echocardiography, hemodynamic evaluation and RV hypertrophy were blinded to the condition, followed an unbiased approach and performed as described previously [38-40].

Statistical analysis
Statistical analyses were performed using Graphpad Prism 7 for Windows (GraphPad Software). Student's t-tests were used for comparisons between two groups. Multiple comparisons were assessed by one-way ANOVA, followed by Bonferroni post-hoc test. p-values < 0.05 were considered significant. All statistical tests used two-sided tests of significance. Data are presented as mean ± SEM.

Results
Nur77 expression is impaired in PAH MVECs
Immunofluorescent staining showed that Nur77 is expressed in ECs, SMCs, fibroblasts, and epithelial cells in the lungs of control, idiopathic PAH (iPAH) and hereditary PAH (HPAH) patients (Fig. 1A). Transcript levels of Nur77 were significantly decreased in lungs of both iPAH and HPAH compared to controls, as shown by qPCR (Fig. 1B). Consistent with this observation, mRNA levels of Nur77 were markedly decreased in cultured human pulmonary microvascular ECs (MVECs) of both iPAH and HPAH compared to controls (Fig. 1C). Furthermore, protein levels of Nur77 were significantly decreased in MVECs of iPAH compared to controls (Fig. 1D). Taken together, these data suggest that Nur77 is involved in PA-EC function in PAH.

Nur77 modulates BMP/SMAD signalling in MVECs
Confirming previous studies, levels of BMPR2 and Id1 were significantly decreased in iPAH MVECs compared to control cells (Fig. 1E). Ectopic expression of Nur77 modestly, but significantly augmented BMPR2 mRNA levels in MVECs (Fig. 1F). Conversely, knock-down of Nur77 decreased BMPR2 protein levels in MVECs (Fig. 1G). To investigate the effect of Nur77 on canonical BMP signalling, we determined the phosphorylation of Smad1/5/8 following ectopic expression of Nur77. Nur77 markedly increased the phosphorylation of Smad1/5/8 under serum, BMP9 and TNFα-stimulated conditions (Fig. 1H). Ectopic expression of Nur77 augmented BMP9-induced BMP/SMAD reporter (BRE-luc) activity [41] (Fig. 1I) and Id3 mRNA expression (Fig. 1J), while knock-down of Nur77 decreased BMP9-induced BRE-luciferase activity in MVECs (Fig. 1K). Nur77 also augmented the expression level of Id1 in PAH MVECs (Fig. 1L). Taken together, our data demonstrated that Nur77 increases BMP/SMAD signalling in MVECs.

Nur77 reduces inflammation of MVECs by inhibiting NFκB activity
As expected, PAH MVECs have higher mRNA levels of the pro-inflammatory cytokines IL-6 and RANTES after TNFα stimulation when compared to control cells (Fig. 2A). Knock-down of Nur77

markedly increased TNFα-induced expression of TNFα, IL-1β and IL-6 at mRNA level (Fig. 2B), while ectopic expression of Nur77 decreased the protein levels of MCP-1 and IL-6 in MVECs (Fig. 2C-D). Furthermore, knock-down of Nur77 significantly increased (Fig. 2E), while ectopic expression of Nur77 strongly decreased the transcriptional activity of the NFκB promoter (Fig. 2F), suggesting that in PA-MVECs Nur77 decreases the expression of pro-inflammatory cytokines through inhibition of the NFκB pathway.

Nur77 attenuates proliferation of MVECs through inhibiting CyclinD1

Both cultured MVECs from control and PAH patients display a cobble stone morphology (Fig. 2G). However, PAH MVECs grow faster as demonstrated by an MTT assay (Fig. 2H). Since Nur77 is reported to decrease cell proliferation by inhibiting CyclinD1 [25], we explored whether loss of Nur77 could explain the hyper-proliferation of PAH MVECs. Over-expression of Nur77 reduced proliferation of both PAH and control MVECs (Fig. 2H), while knock-down of Nur77 stimulated their growth. Furthermore, we found that over-expression of Nur77 decreased (Fig. 2J), while knock-down of Nur77 significantly increased CyclinD1 promoter activity (Fig. 2K). Altogether, these data suggest that Nur77 is involved in PAH MVEC proliferation via modulation of CyclinD1.

Since the interplay between ECs and SMCs is crucial in the pathogenesis of PAH, we next investigated the role of Nur77 in ECs-SMCs interaction. Addition of conditioned medium from TNFα-pre-treated PAH PA-ECs transduced with Nur77 inhibited the growth of healthy PA-SMCs (Fig. 2L), indicating that Nur77 plays an important role not only in PA-ECs but also in the cross-talk between ECs and SMCs.

Nur77 is required for 6-MP-induced activation of BMP signalling

To increase Nur77 activity we stimulated PAH MVECs with two known agonists of Nur77, CsnB and 6-MP [21, 42] and found that both agonists increased the protein levels (Fig. 3A) and mRNA expression of Nur77 (Fig. 3B) in PAH MVECs. Since the transcriptional activity of Nur77 determines its function, we determined the transcriptional activity of Nur77 using a Nur77 specific luciferase reporter (NurRE-luc) [23] in MVECs, and observed that both agonists increased the activity of the Nur77 reporter (Fig. 3C). Interestingly, CsnB and 6-MP also significantly increased the BRE-luc activity (Fig. 3D). To determine whether the observed increase in BRE-luc activity required Nur77, we knocked-down Nur77 and found that both agonists were no longer able to activate the BMP reporter (Fig. 3D). This confirmed our previous observation that Nur77 activates the BMP/Smad signaling pathway. In line with the increased BRE luciferase activity, both agonists also increased the mRNA levels of the down-stream target Id1 (Fig. 3E). Moreover, treatment of PAH MVECs with both agonists decreased proliferation (Fig. 3F) and attenuated CyclinD1-promoter luciferase activity (Fig. 3G). We also found that both CsnB and 6-MP require Nur77 to reduce pro-inflammatory cytokine IL-6 expression (data not shown).Taken together, we show that both CsnB and 6-MP require Nur77, at least partly, to exhibit their function in restoring the behavior of PAH MVECs. Although both agonists of Nur77 displayed similar potential in vitro, we assessed whether 6-MP could prevent development of PH in the SuHx rat model for angioproliferative PH [43], because i) 6-MP is used in the clinic for decades [21, 44], ii) decreased inflammation in cultured MVECs (Supplementary Fig. 1A-B), iii) increased the expression levels of Id3 and BMPR2 in PAH MVECS (Supplementary Fig. 1C-D), and iv) decreased proliferation of healthy human PASMCs (Supplementary Fig. 1E).

6-MP treatment prevents the development of PH

When treating the animals with 1 mg/kg 6-MP per day orally from the start of the experiment till day 42 we found that 6-MP was able to maintain RV function by significantly decreasing RVSP, arterial-elastance (Ea), RV end-diastolic-elastance (stiffness, Eed) while increasing RV-arterial-

coupling (Ees/Ea) (Fig. 4A). Moreover, 6-MP treatment significantly increased stroke volume (SV) and RV systolic function (TAPSE) while significantly decreasing RV free-wall thickness (RVWT) and RV end-diastolic diameter (RVEDD) (Fig. 4B). Consistent with our in vitro findings, 6-MP treatment also decreased serum levels of inflammatory cytokines IL-6 and MCP-1 (Fig. 4C). However, no significant effect of 6-MP on the levels of phospho-IKK α/β was observed (Supplementary Fig. 2A). Furthermore, 6-MP significantly reduced the number of occlusive lesions and fully muscularized arteries, and reduced the thickness of both the intimal and medial layers (Fig. 4D; data not shown). The number of proliferating cells was decreased in 6-MP treated rats compared to vehicle, as determined by immunofluorescent staining for Ki67 (Fig. 4E). Furthermore, 6-MP treatment attenuated the recruitment of CD68 positive macrophages to the lungs (Fig. 4F), while no significant effect of 6-MP on number of B-cells and T-cells was observed (Supplementary Fig. 2B-C). We found no evidence of 6-MP changing the composition of blood cells or systemic blood pressure (Supplementary Fig. 2D; data not shown). Finally, but importantly, RV hypertrophy and RV fibrosis were significantly decreased in the 6-MP-treated PH rats (Fig. 4G-H). Taken together, 6-MP treatment from the start of the experiment prevents the development of PH in the SuHx rat model.

6-MP treatment reverses the development of PH, restores BMP-signalling and increases Nur77 *in vivo*

Before starting 6-MP treatment during disease progression, we first determined the expression levels of Nur77 in the SuHx model, and observed that the expression of Nur77 is increased at initiation of the disease while its expression decreases when disease progresses from week 6 onwards (Supplementary Fig. 3). However, in MCT rats Nur77 levels remained elevated until the usual day of end-experiments: day 21 [25] (data not shown). Therefore, to assess the therapeutic potential of 6-MP in PH, we treated SuHx rats with two doses of 6-MP (1 mg/kg/day and 7.5 mg/kg/day) from day 28 days after the induction of PH. The therapeutic dose of 6-MP (7.5 mg/kg/day) significantly decreased RVSP, Ea, and Eed, but not Ees/Ea (Fig. 5A), while the sub-clinical dose of 6-MP used in the prevention trial (1 mg/kg/day) only significantly decreased Eed, but had no effect on the other parameters (Fig. 5A). The therapeutic dose of 6-MP markedly improved RV function (increase in SV), reduced RV hypertrophy (decrease in RVWT, RVEDD and Fulton index), and suppressed remodelling of the lung vasculature (Fig 5B-D). However, no significant effect of the therapeutic dose of 6-MP was observed on TAPSE, but the sub-clinical dose of 6-MP exhibited an increase in SV and a modest decrease in RVWT and RVEDD (Fig. 5B). Similarly as in the prevention study, the therapeutic dose of 6-MP decreased cell proliferation (number of Ki67 positive cells) (Fig. 5E), RV hypertrophy (cross sectional area) (Fig. 5F), and RV fibrosis (picro sirius staining) (Fig. 5G). In addition, we found that 6-MP significantly increased RV capillary density when compared to the vehicle treated animals (Supplementary Fig. 4). Importantly, we found no evidence of 6-MP affecting blood cell composition or systemic blood pressure (Supplementary Fig. 5A-C; data not shown), but did improve the survival rate of the SuHx rats (Supplementary Fig. 5D).

We next examined the effect of 6-MP treatment on BMP signalling in the lungs of the SuHx rats. In the prevention study, we found that 6-MP increased the expression levels of BMPR2, pSmad1/5/8 and Id3 as demonstrated by immunofluorescent analysis (Fig. 6A-C). Furthermore, 6-MP treatment significantly increased the expression levels of Nur77 in the vessel wall (Fig. 6D). However, no effect of 6-MP on Nur77 in total lung tissue was found as shown by western blot analysis (Supplementary Fig. 6). Consistent with the above findings, therapeutic dose of 6-MP was able to increase the protein levels of BMPR2, pSmad1/5/8, Id1, and Id3 in the reversal study (Fig. 6E-F, Supplementary Fig. 7A). However, no significant effect of 6-MP on phospho-ERK1/2 or apoptosis was observed (Supplementary Fig. 7B-C). Immunofluorescent analysis showed that 6-MP increased the expression levels of Nur77 in the vessel wall (Fig. 6G) while a

modest increase was observed in total lung lysates (Fig. 6E-F). Taken together, 6-MP augmented BMP signaling in vivo, at least partly, via Nur77. We summarized our findings in Figure 6H.

Discussion

The present study demonstrates that down-regulation of Nur77 in the pulmonary vasculature is involved in the pathogenesis of PAH and that activation of Nur77 by 6-MP could be a novel therapeutic option to reverse the abnormal vascular remodelling and RV hypertrophy in PAH. This concept (Fig. 6H) is based on our findings that (i) Nur77 expression is down-regulated in both pulmonary MVECs and lungs of iPAH and HPAH patients; (ii) Absence of Nur77 leads to EC dysfunction and PA-SMC proliferation; (iii) Nur77 suppresses inflammation through inhibition of the NFκB pathway; (iv) pharmacological activation or gain of function of Nur77 inhibits MVEC dysfunction and potently augments BMP/SMAD signalling in MVECs and lungs in vitro and in vivo. Finally, we demonstrated that (v) pharmacological activation of Nur77 attenuates abnormal vascular remodelling and improves RV function in vivo.

Expression of Nur77 has been implicated in several vascular diseases, including atherosclerosis, cardiac hypertrophy, and coronary restenosis [20-28], where Nur77 inhibits proliferation of endothelial cells, smooth muscle cells, pericytes and fibroblasts, while at the same time suppressing inflammation [23, 29, 35, 45]. Proliferation and inflammation are key features of pulmonary vascular remodelling in PAH [13-17]. Several known triggers of PAH such as DNA damage, inflammation, hypoxia, TGFβ signalling, histone acetylation, and disturbed flow have been shown to regulate Nur77 expression and activity in a cell-and context-dependent manner [30, 46-48]. Indeed, in the present study we found that inhibition of HDACs increased Nur77 expression in PAH MVECs (Supplementary Fig. 1F). In addition, post-translational modifications such as phosphorylation and ubiquitination were also shown to regulate Nur77 expression/activity. Indeed, a number of kinases have been shown to phosphorylate and/or interact with Nur77 directly to modulate its activity [22]. Nur77 agonist, 6-MP increases the activity of Nur77 and its family members Nurr1 and NOR-1 via direct modulation of the activation function-1 (AF-1) which is located within the amino terminal-regulatory (A/B) domain of Nur77 [32]. Interestingly, this increase in activity of Nur77 by 6-MP doesn't require the ligand binding domain (LBD) of Nur77. It has also been demonstrated that 6-MP can modulate the activity of the Nur77 coactivator TRAP220 which directly interacts with the AF-1 domain of Nur77 in vivo [49]. Therefore, 6-MP can regulate the expression and activity of Nur77 via direct modulation of the AF-1 domain and/or activation of its coactivator TRAP220 in a cell-and context dependent manner. However, as it is beyond the scope of this study, this has not been investigated in the current study.

A key mechanism by which Nur77 and its agonist 6-MP inhibit cell proliferation is through attenuation of CyclinD1, a known target gene of Nur77 [25, 50, 51]. Indeed, we demonstrated that restoration of Nur77 in PAH MVECs reduced CyclinD1 expression and cellular proliferation. While the role of Nur77 was never before studied in relevant cell populations from patients with PAH, two recent studies demonstrated that Nur77 exhibits anti-proliferative effects in rat PA-SMCs via STAT3/Pim-1/NFAT pathway and human PA-SMCs via the Axin2-beta-catenin signaling pathway [28, 29]. Consistent with this, in the present study we also found that 6-MP directly decreases proliferation of healthy human PASMCs (Supplementary Fig. 1E). The communication between ECs and SMCs plays an essential role in the pathogenesis of PAH. In our study, we found that Nur77 is a key player at the interplay between these cells since the secretome of the diseased PA-ECs stimulates PA-SMC growth. In addition to effects on the EC and SMC proliferation, Nur77 and its activator 6-MP are known to inhibit the NFκB pathway, thereby reducing the production of several cytokines [21, 24, 27]. Here, we confirm that 6-MP decreases the secretion of inflammatory cytokines in pulmonary MVECs and also in serum and lung tissue of the 6-MP treated SuHx rats.

While the effects of Nur77 on vascular proliferation and inflammation were possibly exerted through interaction with multiple pathways, we provide first evidence that at least some of this effect in PAH is through control of the BMPR2 gene. Germline mutations in BMPR2 is the strongest known genetic risk factor associated with PAH; about 40% of all subjects carrying mutations resulting in haplo-insufficiency will ultimately develop HPAH [4, 17, 44, 52, 53]. Even in iPAH patients both BMPR2 and BMP signalling are reduced [4, 6]. Loss of BMPR2 has been linked to increased inflammation and proliferation of pulmonary ECs, and it has been suggested that restoring BMP signalling might be beneficial for the treatment of PAH patients [18, 19]. Indeed, enhanced BMP signalling by BMP9 treatment reduced the development of PAH in animal models [37]. Previously, Nur77 was shown to modulate TGFβ signalling in a cell- and context-dependent manner [30, 31]. Our data provides the first in vitro and in vivo evidence that Nur77 controls BMP signalling as well. Our findings imply that Nur77, via the BMPR2-Smad-Id1 axis, may significantly promote EC function in HPAH and iPAH. Therefore, activation of Nur77 can serve as a novel therapeutic approach for HPAH and other PAH patients with impaired BMP signalling.

Whether using a prevention or reversal strategy, oral administration of 6-MP markedly reduced RVSP and improved RV function in the SuHx PH rat model. The hemodynamic effects of 6-MP were associated with markedly reduced proliferation and inflammation and reversed abnormal vascular remodelling. Crucially, the beneficial effect of 6-MP was associated with normalization of Nur77 expression and BMP signalling. Taking into account the observed beneficial effect of 6-MP in SuHx rats in this short treatment period, prolonged treatment with 6-MP may even result in a stronger reversal of PAH. Importantly, we observed no immunosuppression at the dose given in the 6-MP treated animals in both the prevention and reversal study. Although no side effects were observed in these preclinical models and 6-MP is already used in several clinical conditions in patients [21, 35, 44], future research should focus on testing 6-MP in combination with other PAH drugs as well as the development of lung-specific delivery methods [54] to achieve efficient pulmonary efficacy at low drug concentrations.

Despite recent advances in PAH research, there is still no cure for this deadly disease. EC dysfunction is a crucial element in the initiation and pathogenesis of PAH and our data provide evidence that Nur77 is a novel positive regulator of pulmonary MVEC function and thereby inhibits adverse vascular remodelling in PAH. Specifically, Nur77 exhibits significant anti-proliferative and anti-inflammatory effects and augments BMP signalling in vitro and in vivo. In conclusion, 6-MP displays beneficial effects in vitro and in vivo, and this well-known drug provides an innovative treatment opportunity for patients suffering from the so far untreatable disease PAH.

Acknowledgments
We thank Martijn Rabelink for providing shRNAs targeting Nur77.

Support statement: We acknowledge support from the Netherlands CardioVascular Research Initiative: the Dutch Heart Foundation, Dutch Federation of University Medical Centers, the Netherlands Organization for Health Research and Development, and the Royal Netherlands Academy of Sciences Grant 2012-08 awarded to the Phaedra consortium (http://www.phaedraresearch.nl). We also acknowledge support for KK by the Grants4Targets (Bayer AG) grant number-2016-03-1554 and by the Dutch Lung Foundation (Longfonds) grant number-5.2.17.198J0.

Disclosures
None

References

1. Tuder RM, Archer SL, Dorfmuller P, Erzurum SC, Guignabert C, Michelakis E, Rabinovitch M, Schermuly R, Stenmark KR, Morrell NW. Relevant issues in the pathology and pathobiology of pulmonary hypertension. *Journal of the American College of Cardiology* 2013: 62(25 Suppl): D4-12.
2. D'Alonzo GE, Barst RJ, Ayres SM, Bergofsky EH, Brundage BH, Detre KM, Fishman AP, Goldring RM, Groves BM, Kernis JT, et al. Survival in patients with primary pulmonary hypertension. Results from a national prospective registry. *Annals of internal medicine* 1991: 115(5): 343-349.
3. Galie N, Humbert M, Vachiery JL, Gibbs S, Lang I, Torbicki A, Simonneau G, Peacock A, Vonk Noordegraaf A, Beghetti M, Ghofrani A, Gomez Sanchez MA, Hansmann G, Klepetko W, Lancellotti P, Matucci M, McDonagh T, Pierard LA, Trindade PT, Zompatori M, Hoeper M, Aboyans V, Vaz Carneiro A, Achenbach S, Agewall S, Allanore Y, Asteggiano R, Paolo Badano L, Albert Barbera J, Bouvaist H, Bueno H, Byrne RA, Carerj S, Castro G, Erol C, Falk V, Funck-Brentano C, Gorenflo M, Granton J, Iung B, Kiely DG, Kirchhof P, Kjellstrom B, Landmesser U, Lekakis J, Lionis C, Lip GY, Orfanos SE, Park MH, Piepoli MF, Ponikowski P, Revel MP, Rigau D, Rosenkranz S, Voller H, Luis Zamorano J. 2015 ESC/ERS Guidelines for the diagnosis and treatment of pulmonary hypertension: The Joint Task Force for the Diagnosis and Treatment of Pulmonary Hypertension of the European Society of Cardiology (ESC) and the European Respiratory Society (ERS): Endorsed by: Association for European Paediatric and Congenital Cardiology (AEPC), International Society for Heart and Lung Transplantation (ISHLT). *Eur Heart J* 2016: 37(1): 67-119.
4. Morrell NW, Adnot S, Archer SL, Dupuis J, Jones PL, MacLean MR, McMurtry IF, Stenmark KR, Thistlethwaite PA, Weissmann N, Yuan JX, Weir EK. Cellular and molecular basis of pulmonary arterial hypertension. *Journal of the American College of Cardiology* 2009: 54(1 Suppl): S20-31.
5. Yang J, Davies RJ, Southwood M, Long L, Yang X, Sobolewski A, Upton PD, Trembath RC, Morrell NW. Mutations in bone morphogenetic protein type II receptor cause dysregulation of Id gene expression in pulmonary artery smooth muscle cells: implications for familial pulmonary arterial hypertension. *Circulation research* 2008: 102(10): 1212-1221.
6. Atkinson C, Stewart S, Upton PD, Machado R, Thomson JR, Trembath RC, Morrell NW. Primary pulmonary hypertension is associated with reduced pulmonary vascular expression of type II bone morphogenetic protein receptor. *Circulation* 2002: 105(14): 1672-1678.
7. Voelkel NF, Gomez-Arroyo J, Abbate A, Bogaard HJ, Nicolls MR. Pathobiology of pulmonary arterial hypertension and right ventricular failure. *Eur Respir J* 2012: 40(6): 1555-1565.
8. Perros F, Bonnet S. Bone morphogenetic protein receptor type II and inflammation are bringing old concepts into the new pulmonary arterial hypertension world. *American journal of respiratory and critical care medicine* 2015: 192(7): 777-779.
9. Alastalo TP, Li M, Perez Vde J, Pham D, Sawada H, Wang JK, Koskenvuo M, Wang L, Freeman BA, Chang HY, Rabinovitch M. Disruption of PPARgamma/beta-catenin-mediated regulation of apelin impairs BMP-induced mouse and human pulmonary arterial EC survival. *The Journal of clinical investigation* 2011: 121(9): 3735-3746.
10. Hong KH, Lee YJ, Lee E, Park SO, Han C, Beppu H, Li E, Raizada MK, Bloch KD, Oh SP. Genetic ablation of the BMPR2 gene in pulmonary endothelium is sufficient to predispose to pulmonary arterial hypertension. *Circulation* 2008: 118(7): 722-730.
11. Yuan K, Shao NY, Hennigs JK, Discipulo M, Orcholski ME, Shamskhou E, Richter A, Hu X, Wu JC, de Jesus Perez VA. Increased Pyruvate Dehydrogenase Kinase 4 Expression in Lung Pericytes Is Associated with Reduced Endothelial-Pericyte Interactions and Small Vessel

Loss in Pulmonary Arterial Hypertension. *The American journal of pathology* 2016: 186(9): 2500-2514.
12. Zhang H, Wang D, Li M, Plecita-Hlavata L, D'Alessandro A, Tauber J, Riddle S, Kumar S, Flockton AR, McKeon BA, Frid MG, Reisz JA, Caruso P, El Kasmi KC, Jezek P, Morrell NW, Hu CJ, Stenmark KR. The Metabolic and Proliferative State of Vascular Adventitial Fibroblasts in Pulmonary Hypertension is Regulated through a MiR-124/PTBP1/PKM Axis. *Circulation* 2017.
13. Le Hiress M, Tu L, Ricard N, Phan C, Thuillet R, Fadel E, Dorfmuller P, Montani D, de Man F, Humbert M, Huertas A, Guignabert C. Proinflammatory Signature of the Dysfunctional Endothelium in Pulmonary Hypertension. Role of the Macrophage Migration Inhibitory Factor/CD74 Complex. *American journal of respiratory and critical care medicine* 2015: 192(8): 983-997.
14. Meloche J, Renard S, Provencher S, Bonnet S. Anti-inflammatory and immunosuppressive agents in PAH. *Handbook of experimental pharmacology* 2013: 218: 437-476.
15. Savai R, Pullamsetti SS, Kolbe J, Bieniek E, Voswinckel R, Fink L, Scheed A, Ritter C, Dahal BK, Vater A, Klussmann S, Ghofrani HA, Weissmann N, Klepetko W, Banat GA, Seeger W, Grimminger F, Schermuly RT. Immune and inflammatory cell involvement in the pathology of idiopathic pulmonary arterial hypertension. *American journal of respiratory and critical care medicine* 2012: 186(9): 897-908.
16. Toshner M, Voswinckel R, Southwood M, Al-Lamki R, Howard LS, Marchesan D, Yang J, Suntharalingam J, Soon E, Exley A, Stewart S, Hecker M, Zhu Z, Gehling U, Seeger W, Pepke-Zaba J, Morrell NW. Evidence of dysfunction of endothelial progenitors in pulmonary arterial hypertension. *American journal of respiratory and critical care medicine* 2009: 180(8): 780-787.
17. Voelkel NF, Tamosiuniene R, Nicolls MR. Challenges and opportunities in treating inflammation associated with pulmonary hypertension. *Expert review of cardiovascular therapy* 2016: 14(8): 939-951.
18. Majka S, Hagen M, Blackwell T, Harral J, Johnson JA, Gendron R, Paradis H, Crona D, Loyd JE, Nozik-Grayck E, Stenmark KR, West J. Physiologic and molecular consequences of endothelial Bmpr2 mutation. *Respiratory research* 2011: 12: 84.
19. Xiong J. BMPR2 spruces up the endothelium in pulmonary hypertension. *Protein & cell* 2015: 6(10): 703-708.
20. Kurakula K, Hamers AA, de Waard V, de Vries CJ. Nuclear Receptors in atherosclerosis: a superfamily with many 'Goodfellas'. *Molecular and cellular endocrinology* 2013: 368(1-2): 71-84.
21. Kurakula K, Hamers AA, van Loenen P, de Vries CJ. 6-Mercaptopurine reduces cytokine and Muc5ac expression involving inhibition of NFkappaB activation in airway epithelial cells. *Respiratory research* 2015: 16: 73.
22. Kurakula K, Koenis DS, van Tiel CM, de Vries CJ. NR4A nuclear receptors are orphans but not lonesome. *Biochimica et biophysica acta* 2014: 1843(11): 2543-2555.
23. Kurakula K, van der Wal E, Geerts D, van Tiel CM, de Vries CJ. FHL2 protein is a novel co-repressor of nuclear receptor Nur77. *The Journal of biological chemistry* 2011: 286(52): 44336-44343.
24. Kurakula K, Vos M, Logiantara A, Roelofs JJ, Nieuwenhuis MA, Koppelman GH, Postma DS, van Rijt LS, de Vries CJ. Nuclear Receptor Nur77 Attenuates Airway Inflammation in Mice by Suppressing NF-kappaB Activity in Lung Epithelial Cells. *Journal of immunology (Baltimore, Md : 1950)* 2015: 195(4): 1388-1398.
25. Liu Y, Zhang J, Yi B, Chen M, Qi J, Yin Y, Lu X, Jasmin JF, Sun J. Nur77 suppresses pulmonary artery smooth muscle cell proliferation through inhibition of the STAT3/Pim-1/NFAT pathway. *American journal of respiratory cell and molecular biology* 2014: 50(2): 379-388.

26. Medzikovic L, Schumacher CA, Verkerk AO, van Deel ED, Wolswinkel R, van der Made I, Bleeker N, Cakici D, van den Hoogenhof MM, Meggouh F, Creemers EE, Remme CA, Baartscheer A, de Winter RJ, de Vries CJ, Arkenbout EK, de Waard V. Orphan nuclear receptor Nur77 affects cardiomyocyte calcium homeostasis and adverse cardiac remodelling. *Scientific reports* 2015: 5: 15404.
27. Qin Q, Chen M, Yi B, You X, Yang P, Sun J. Orphan nuclear receptor Nur77 is a novel negative regulator of endothelin-1 expression in vascular endothelial cells. *Journal of molecular and cellular cardiology* 2014: 77: 20-28.
28. You B, Jiang YY, Chen S, Yan G, Sun J. The orphan nuclear receptor Nur77 suppresses endothelial cell activation through induction of IkappaBalpha expression. *Circulation research* 2009: 104(6): 742-749.
29. Nie X, Tan J, Dai Y, Mao W, Chen Y, Qin G, Li G, Shen C, Zhao J, Chen J. Nur77 downregulation triggers pulmonary artery smooth muscle cell proliferation and migration in mice with hypoxic pulmonary hypertension via the Axin2-beta-catenin signaling pathway. *Vascular pharmacology* 2016: 87: 230-241.
30. Palumbo-Zerr K, Zerr P, Distler A, Fliehr J, Mancuso R, Huang J, Mielenz D, Tomcik M, Furnrohr BG, Scholtysek C, Dees C, Beyer C, Kronke G, Metzger D, Distler O, Schett G, Distler JH. Orphan nuclear receptor NR4A1 regulates transforming growth factor-beta signaling and fibrosis. *Nature medicine* 2015: 21(2): 150-158.
31. Zhou F, Drabsch Y, Dekker TJ, de Vinuesa AG, Li Y, Hawinkels LJ, Sheppard KA, Goumans MJ, Luwor RB, de Vries CJ, Mesker WE, Tollenaar RA, Devilee P, Lu CX, Zhu H, Zhang L, Dijke PT. Nuclear receptor NR4A1 promotes breast cancer invasion and metastasis by activating TGF-beta signalling. *Nature communications* 2014: 5: 3388.
32. Wansa KD, Harris JM, Yan G, Ordentlich P, Muscat GE. The AF-1 domain of the orphan nuclear receptor NOR-1 mediates trans-activation, coactivator recruitment, and activation by the purine anti-metabolite 6-mercaptopurine. *The Journal of biological chemistry* 2003: 278(27): 24776-24790.
33. Marinkovic G, Kroon J, Hoogenboezem M, Hoeben KA, Ruiter MS, Kurakula K, Otermin Rubio I, Vos M, de Vries CJ, van Buul JD, de Waard V. Inhibition of GTPase Rac1 in endothelium by 6-mercaptopurine results in immunosuppression in nonimmune cells: new target for an old drug. *Journal of immunology (Baltimore, Md : 1950)* 2014: 192(9): 4370-4378.
34. Weigel G, Griesmacher A, DeAbreu RA, Wolner E, Mueller MM. Azathioprine and 6-mercaptopurine alter the nucleotide balance in endothelial cells. *Thrombosis research* 1999: 94(2): 87-94.
35. Pires NM, Pols TW, de Vries MR, van Tiel CM, Bonta PI, Vos M, Arkenbout EK, Pannekoek H, Jukema JW, Quax PH, de Vries CJ. Activation of nuclear receptor Nur77 by 6-mercaptopurine protects against neointima formation. *Circulation* 2007: 115(4): 493-500.
36. Szulcek R, Happe CM, Rol N, Fontijn RD, Dickhoff C, Hartemink KJ, Grunberg K, Tu L, Timens W, Nossent GD, Paul MA, Leyen TA, Horrevoets AJ, de Man FS, Guignabert C, Yu PB, Vonk-Noordegraaf A, van Nieuw Amerongen GP, Bogaard HJ. Delayed Microvascular Shear Adaptation in Pulmonary Arterial Hypertension. Role of Platelet Endothelial Cell Adhesion Molecule-1 Cleavage. *American journal of respiratory and critical care medicine* 2016: 193(12): 1410-1420.
37. Long L, Ormiston ML, Yang X, Southwood M, Graf S, Machado RD, Mueller M, Kinzel B, Yung LM, Wilkinson JM, Moore SD, Drake KM, Aldred MA, Yu PB, Upton PD, Morrell NW. Selective enhancement of endothelial BMPR-II with BMP9 reverses pulmonary arterial hypertension. *Nature medicine* 2015: 21(7): 777-785.
38. da Silva Goncalves Bos D, Van Der Bruggen CE, Kurakula K, Sun XQ, Casali KR, Casali AG, Rol N, Szulcek R, Dos Remedios C, Guignabert C, Tu L, Dorfmuller P, Humbert M, Wijnker PJM, Kuster DWD, van der Velden J, Goumans MJ, Bogaard HJ, Vonk-Noordegraaf A, de Man FS, Handoko ML. Contribution of Impaired Parasympathetic Activity to Right Ventricular

Dysfunction and Pulmonary Vascular Remodeling in Pulmonary Arterial Hypertension. *Circulation* 2017.
39. de Raaf MA, Kroeze Y, Middelman A, de Man FS, de Jong H, Vonk-Noordegraaf A, de Korte C, Voelkel NF, Homberg J, Bogaard HJ. Serotonin transporter is not required for the development of severe pulmonary hypertension in the Sugen hypoxia rat model. *Am J Physiol Lung Cell Mol Physiol* 2015: 309(10): L1164-1173.
40. Provencher S, Archer SL, Ramirez FD, Hibbert B, Paulin R, Boucherat O, Lacasse Y, Bonnet S. Standards and Methodological Rigor in Pulmonary Arterial Hypertension Preclinical and Translational Research. *Circulation research* 2018: 122(7): 1021-1032.
41. Korchynskyi O, ten Dijke P. Identification and functional characterization of distinct critically important bone morphogenetic protein-specific response elements in the Id1 promoter. *The Journal of biological chemistry* 2002: 277(7): 4883-4891.
42. Zhan Y, Du X, Chen H, Liu J, Zhao B, Huang D, Li G, Xu Q, Zhang M, Weimer BC, Chen D, Cheng Z, Zhang L, Li Q, Li S, Zheng Z, Song S, Huang Y, Ye Z, Su W, Lin SC, Shen Y, Wu Q. Cytosporone B is an agonist for nuclear orphan receptor Nur77. *Nature chemical biology* 2008: 4(9): 548-556.
43. Taraseviciene-Stewart L, Kasahara Y, Alger L, Hirth P, Mc Mahon G, Waltenberger J, Voelkel NF, Tuder RM. Inhibition of the VEGF receptor 2 combined with chronic hypoxia causes cell death-dependent pulmonary endothelial cell proliferation and severe pulmonary hypertension. *FASEB journal : official publication of the Federation of American Societies for Experimental Biology* 2001: 15(2): 427-438.
44. Domenech E, Nos P, Papo M, Lopez-San Roman A, Garcia-Planella E, Gassull MA. 6-mercaptopurine in patients with inflammatory bowel disease and previous digestive intolerance of azathioprine. *Scandinavian journal of gastroenterology* 2005: 40(1): 52-55.
45. Huo Y, Yi B, Chen M, Wang N, Chen P, Guo C, Sun J. Induction of Nur77 by hyperoside inhibits vascular smooth muscle cell proliferation and neointimal formation. *Biochemical pharmacology* 2014: 92(4): 590-598.
46. To SK, Zeng WJ, Zeng JZ, Wong AS. Hypoxia triggers a Nur77-beta-catenin feed-forward loop to promote the invasive growth of colon cancer cells. *British journal of cancer* 2014: 110(4): 935-945.
47. Xie X, Song X, Yuan S, Cai H, Chen Y, Chang X, Liang B, Huang D. Histone acetylation regulates orphan nuclear receptor NR4A1 expression in hypercholesterolaemia. *Clinical science (London, England : 1979)* 2015: 129(12): 1151-1161.
48. Dequiedt F, Kasler H, Fischle W, Kiermer V, Weinstein M, Herndier BG, Verdin E. HDAC7, a thymus-specific class II histone deacetylase, regulates Nur77 transcription and TCR-mediated apoptosis. *Immunity* 2003: 18(5): 687-698.
49. Wansa KD, Muscat GE. TRAP220 is modulated by the antineoplastic agent 6-Mercaptopurine, and mediates the activation of the NR4A subgroup of nuclear receptors. *Journal of molecular endocrinology* 2005: 34(3): 835-848.
50. Marinkovic G, Kroon J, Hoogenboezem M, Hoeben KA, Ruiter MS, Kurakula K, Otermin Rubio I, Vos M, de Vries CJ, van Buul JD, de Waard V. Inhibition of GTPase Rac1 in endothelium by 6-mercaptopurine results in immunosuppression in nonimmune cells: new target for an old drug. *Journal of immunology (Baltimore, Md : 1950)* 2014: 192(9): 4370-4378.
51. Nomiyama T, Zhao Y, Gizard F, Findeisen HM, Heywood EB, Jones KL, Conneely OM, Bruemmer D. Deficiency of the NR4A neuron-derived orphan receptor-1 attenuates neointima formation after vascular injury. *Circulation* 2009: 119(4): 577-586.
52. Deng Z, Morse JH, Slager SL, Cuervo N, Moore KJ, Venetos G, Kalachikov S, Cayanis E, Fischer SG, Barst RJ, Hodge SE, Knowles JA. Familial primary pulmonary hypertension (gene PPH1) is caused by mutations in the bone morphogenetic protein receptor-II gene. *American journal of human genetics* 2000: 67(3): 737-744.

53. van der Bruggen CE, Happe CM, Dorfmuller P, Trip P, Spruijt OA, Rol N, Hoevenaars FP, Houweling AC, Girerd B, Marcus JT, Mercier O, Humbert M, Handoko ML, van der Velden J, Vonk Noordegraaf A, Bogaard HJ, Goumans MJ, de Man FS. Bone Morphogenetic Protein Receptor Type 2 Mutation in Pulmonary Arterial Hypertension: A View on the Right Ventricle. *Circulation* 2016: 133(18): 1747-1760.
54. Yin Y, Wu X, Yang Z, Zhao J, Wang X, Zhang Q, Yuan M, Xie L, Liu H, He Q. The potential efficacy of R8-modified paclitaxel-loaded liposomes on pulmonary arterial hypertension. *Pharmaceutical research* 2013: 30(8): 2050-2062.

Figure 1

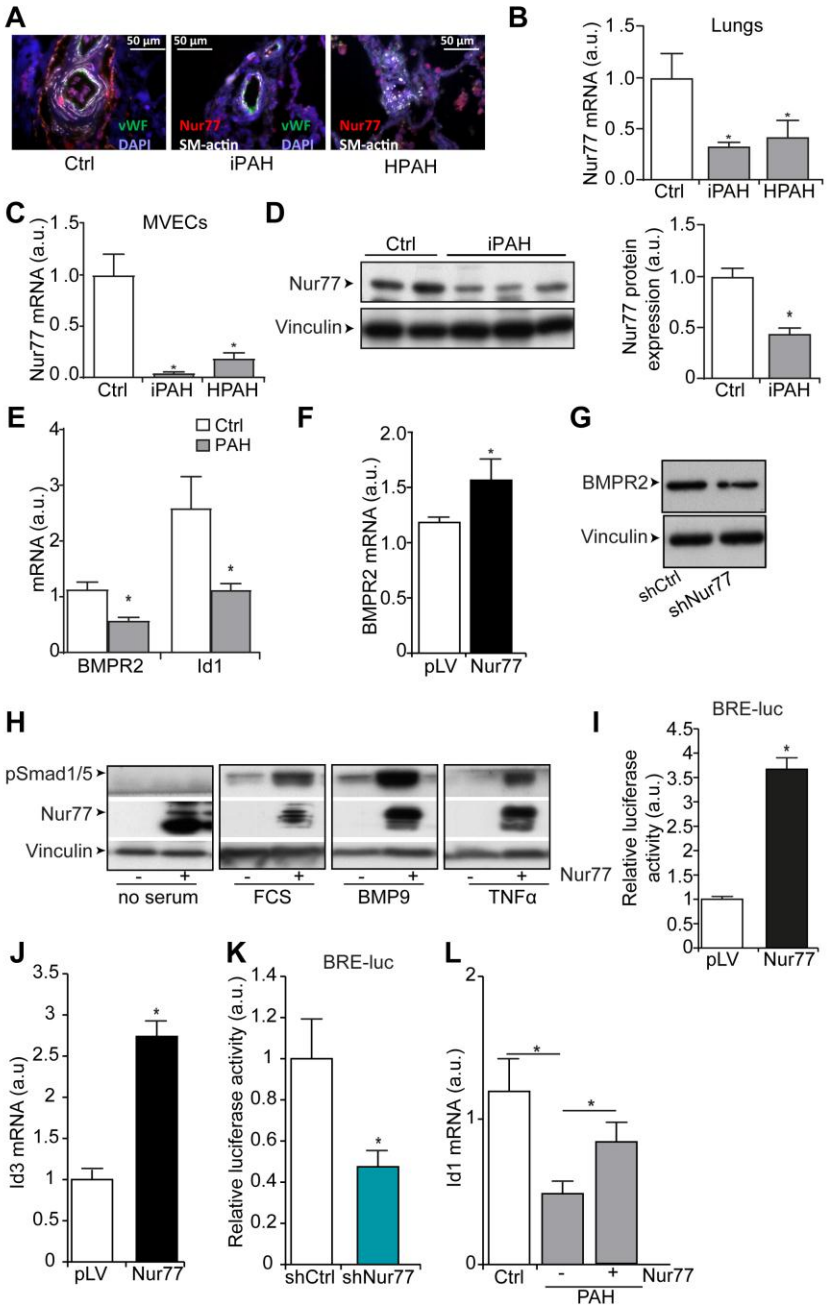

Figure 1: Nur77 expression is reduced in PAH and Nur77 enhances BMP signalling in microvascular ECs. (A) Representative immunofluorescence photomicrographs of Nur77 (red), Von Willebrand factor (vWF, green) and α-smooth muscle actin (SM-actin, white) in human pulmonary arteries from control, iPAH and HPAH lungs (n=4). DAPI (blue). **(B-C)** qRT-PCR was performed to assess mRNA expression of Nur77 in control, iPAH and HPAH lungs (n=6 per group) (B), and in MVECs from control, iPAH and HPAH patients (n=4 per group) (C). **(D)** Representative western blots with relative densitometric analyses showing Nur77 in total lung form control and iPAH patients. **(E)** qRT-PCR was performed to assess mRNA expression of BMPR2 and Id1 in MVECs from control and PAH patients (n=6 per group). **(F)** qRT-PCR was performed to assess mRNA expression of BMPR2 in MVECs, following overexpression of Nur77 (n=3). **(G)** Representative western blots (n=3) showing BMPR2 in MVECs following knock-down of Nur77 by shNur77 lentivirus. **(H)** Representative western blots showing pSMAD1/5 following overexpression of Nur77 and stimulation with vehicle (Veh), serum (10%), BMP9 (1 ng/mL), TNFα (50 ng/ml) in MVECs (n=3). **(I)** BRE-luciferase activity in MVECs was measured following overexpression of Nur77 and stimulation with BMP9 (1ng/ml) for 16 h (n=3). **(J)** qRT-PCR was performed to assess mRNA expression of Id3 in MVECs, following ectopic expression of Nur77 (n=3). **(K)** BRE-luciferase activity in MVECs was measured following knock-down of Nur77 and stimulation with BMP9 (1ng/ml) for 16 h (n=3). **(L)** qRT-PCR was performed to assess mRNA expression of Id1 in control and PAH MVECs, following ectopic expression of Nur77 (n=3). *p<0.05. Student's t-test was used for comparisons between two groups. Multiple comparisons were assessed by one-way ANOVA, followed by Bonferroni post-hoc test. Error bars, mean ± s.e.m.

Figure 2

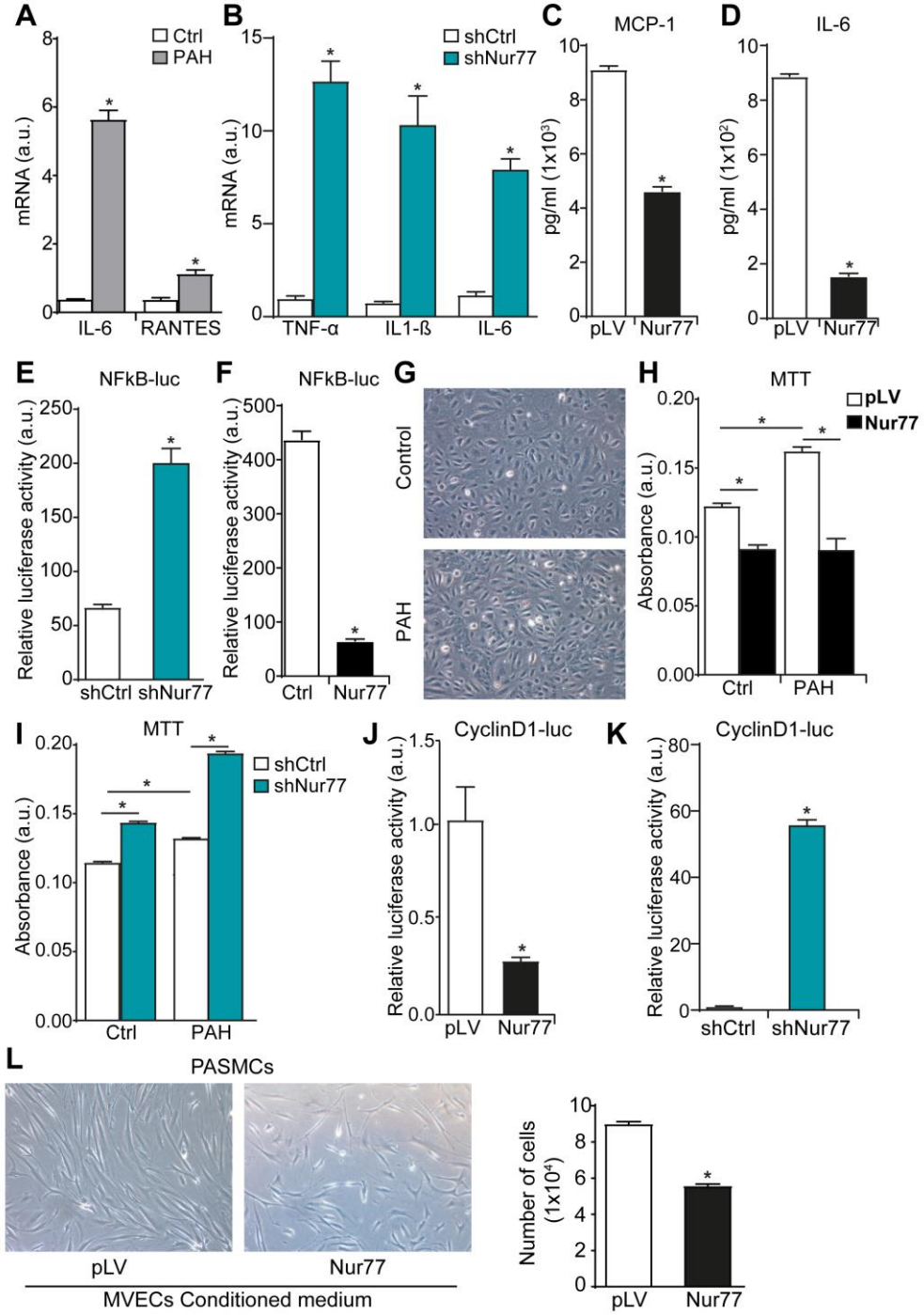

Figure 2: Nur77 inhibits inflammation and proliferation of MVECs. (A) qRT-PCR was performed to assess mRNA expression of IL-6 and RANTES in TNFα- stimulated MVECs (6 h) from control and iPAH patients (n=3). **(B)** qRT-PCR was performed to assess mRNA expression of TNFα, IL-1β and IL-6 in TNFα- stimulated MVECs (6 h) (n=3). **(C-D)** ELISAs for MCP-1 (C) and IL-6 (D) were performed using supernatants from MVECs following ectopic expression of Nur77 and stimulation with TNFα for 6 h (n=4). **(E-F)** TNFα induced NFκB-luciferase activity in HEK293T cells was measured following knock-down (E) and ectopic expression of Nur77 (F) (n=3). **(G)** Morphological appearance of control and PAH MVECs. **(H-I)** MTT assays were performed to assess proliferation of control and PAH MVECs following knock-down (H) and ectopic expression of Nur77 (n=3) (I). **(J-K)** CyclinD1 promoter luciferase activity in HEK293T cells was measured following ectopic expression (J) and knock-down of Nur77 (K). The data shown are representative of three experiments. **(L)** Assessment of serum starved SMC proliferation following incubation with conditioned medium from PAH MVECs without and with ectopically expressed Nur77 and stimulated with TNFα (n=3). **p<0.05. Student's t-tests were used for comparisons between two groups. Multiple comparisons were assessed by one-way ANOVA, followed by Bonferroni post-hoc test. Error bars, mean ± s.e.m.

Figure 3

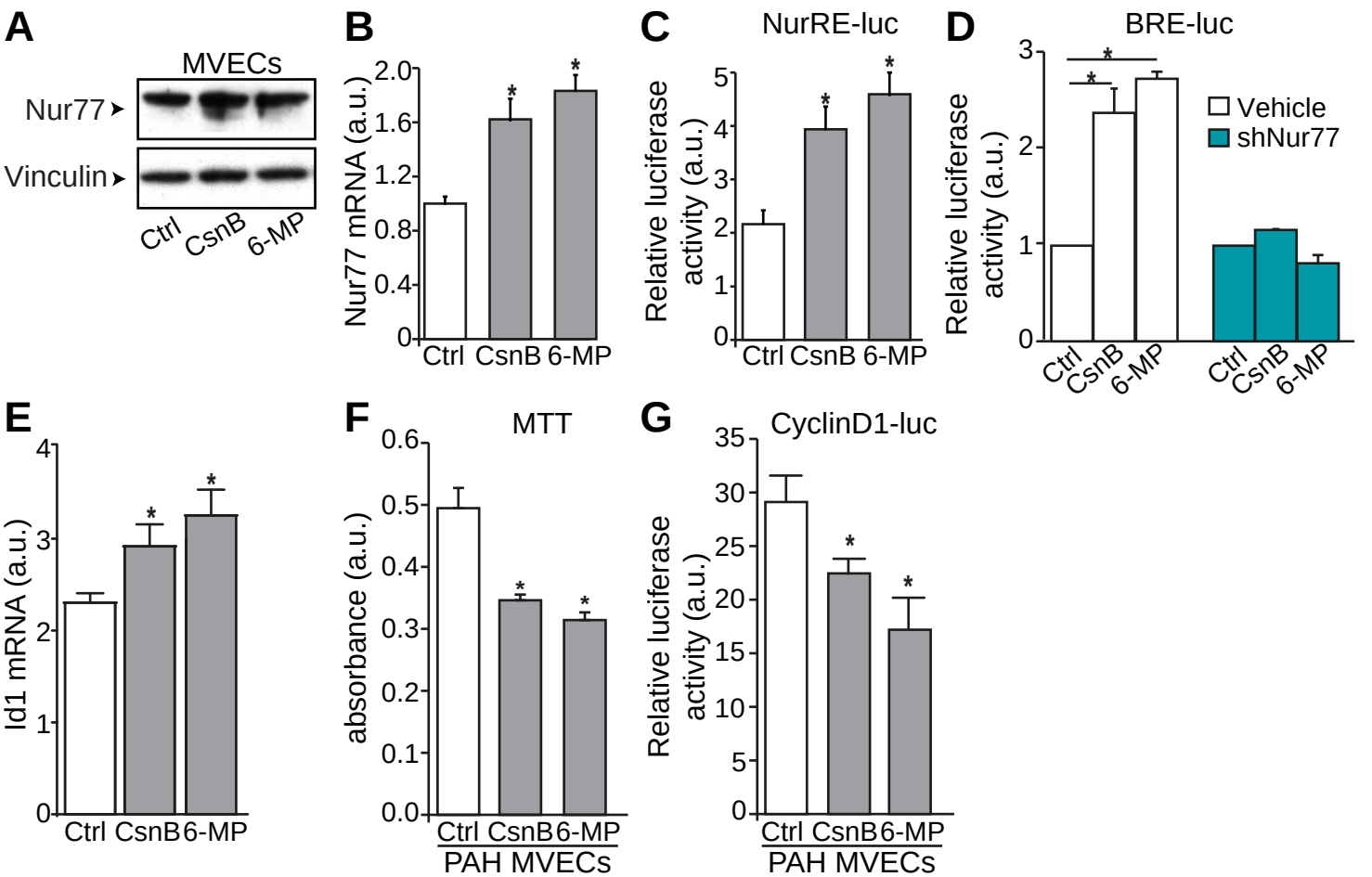

Figure 3: Upregulated Nur77 is involved in the 6-MP-mediated effect on BMP signalling in MVECs. **(A-B)** Western blot (n=3) (A) and qRT-PCR (n=3) analysis (B) was performed to measure the expression of Nur77 in MVECs that were pre-treated with CsnB (5 uM) or 6-MP (10 uM) for 16 h. **(C)** The activity of Nur77 was monitored in MVECs expressing the NurRE-luc reporter following treatment with CsnB (5 uM) or 6-MP (10 uM). The data shown are representative of three experiments. **(D)** Overall BRE-luciferase activity was measured in MVECs transduced with control or shNur77 lentivirus for 48 h followed by treatment with CsnB (5 uM) or 6-MP (10 uM) in the presence of BMP9 (1 ng/ml) for 16 h (n=3). **(E)** qRT-PCR was performed to assess mRNA expression of Id1 following treatment with CsnB (5 uM) or 6-MP (10 uM) for 16 h (n=3). **(F)** MTT assays were performed to assess PAH MVEC proliferation following treatment with CsnB (5 uM) or 6-MP (10 uM) for 24 h (n=3). **(G)** CyclinD1 promoter luciferase activity in PAH MVECs was measured following treatment with CsnB (5 uM) or 6-MP (10 uM) for 16 h (n=3). *p<0.05. Multiple comparisons were assessed by one-way ANOVA, followed by Bonferroni post-hoc test. Error bars, mean ± s.e.m.

Figure 4

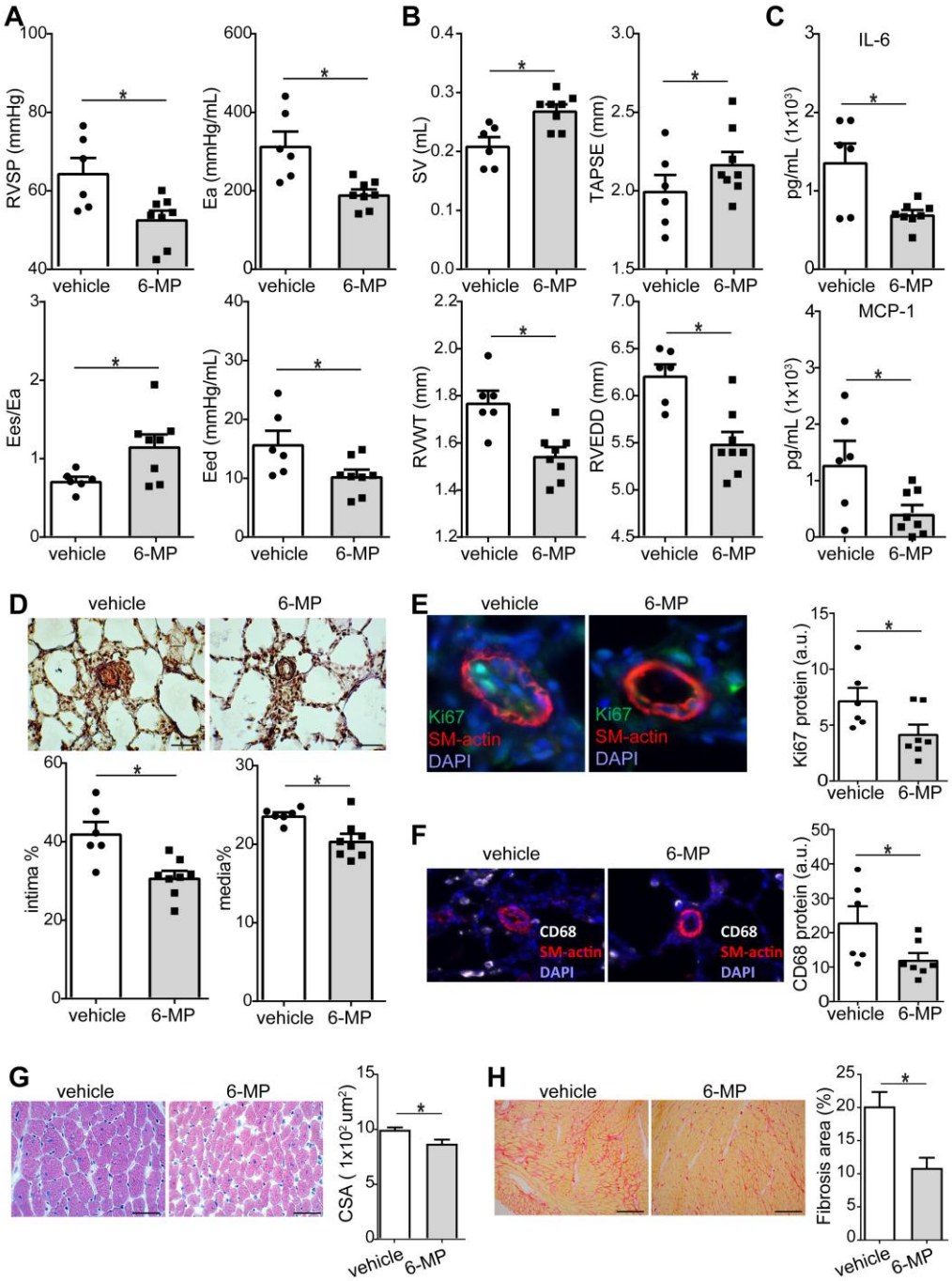

Figure 4: 6-MP prevents the development of PH and improves cardiac function in SuHx-induced PH in rats. (A) SuHx rats were treated with 6-MP in drinking water from the start till the end of the experiment. Echocardiography, followed by physiological measurements, was carried out at the day of termination (day 42). RVSP (top left), Ea (top right), Ees/Ea (bottom left) and Eed (bottom right) are shown for the indicated groups of rats. n=6 rats for vehicle and n=8 for 6-MP-treated SuHx per group. **(B)** SV (top left), TAPSE (top right), RVWT(bottom left), and RVEDD (bottom right) are shown for the indicated groups. n = 6-8 lungs per group. **(C)** ELISAs for IL-6 (top panel) and MCP-1 (bottom panel) were performed in serum from the indicated groups. n = 6-8 lungs per group. **(D)** The neointima to media ratio of pulmonary arteries (<90 µm in diameter) from lung sections of SuHx-treated rats was determined by morphometric analysis of pulmonary vessels following Elastica van Giesson staining. n = 6-8 lungs per group. Scale bar: 20 µm. **(E-F)** Immunofluorescent staining for Ki67 (green) (E) and CD68 (white) (F) were performed in small pulmonary arteries from vehicle and 6-MP treated rats. SM-actin (red) and nuclei (DAPI) were co-stained with Ki67 or CD68. Quantification of the fluorescence is shown in the bar graph next to the images. The images are representative of n = 6-8 lungs per group. **(G)** Mean cardiomyocyte cross-sectional area (CSA) was assessed in the RV from vehicle and 6-MP treated rats following Haematoxylin and Eosin staining. Scale bar: 20 µm. Quantification of CSA is shown in the bar graph next to the images. n = 6-8 lungs per group. **(H)** Picrosirius red staining was performed to assess the fibrosis in the RV from control and 6-MP treated rats. Scale bar: 80 µm. Quantification of fibrosis is shown in the bar graph next to the images. n = 6-8 lungs per group. RVSP: right ventricular systolic pressure, Ea: arterial elastance, TAPSE: tricuspid annular plane systolic excursion, Eed: end-diastolic elastance, RVWT: right ventricular wall thickness, RVEDD: right ventricular end diastolic diameter, SV: stroke volume. *p<0.05. Student's t-tests were used for comparisons between two groups. Error bars, mean ± s.e.m.

Figure 5

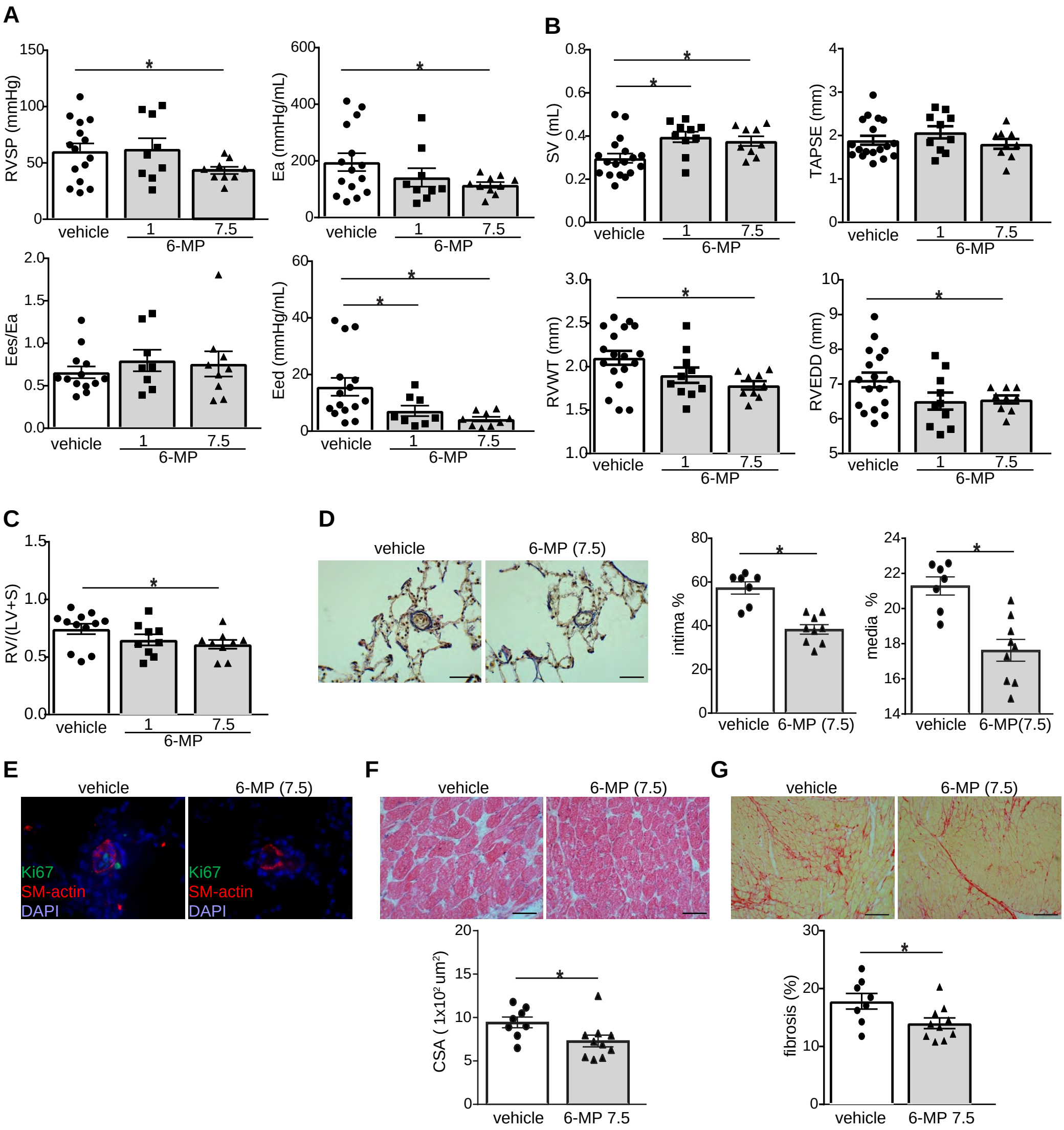

Figure 5: 6-MP reverses pulmonary vascular remodelling and pulmonary hypertension in SuHx-induced PH in rats. (A) Two concentrations (1 mg/kg/day and 7.5 mg/kg/day) of 6-MP was administered in the drinking water from days 42 to 70 to SuHx rats after randomization. Echocardiography, followed by physiological measurements, was carried out at the day of termination (day 70). RVSP (top left), Ea (top right), Ees/Ea (bottom left) and Eed (bottom right) are shown for the indicated groups of rats. n=14 rats for vehicle or n=9 for 6-MP-1 mg or n=9 for 6-MP-7.5 mg per group. **(B)** SV (top left), TAPSE (top right), RVWT (bottom left), and RVEDD (bottom right) are shown for the indicated groups. **(C)** RV hypertrophy, defined by the Fulton index, weight of RV/left ventricle + septum (LV+S) was measured. n = 9-14 rats per group. **(D)** The neointima to media ratio of pulmonary arteries (<90 µm in diameter) from lung sections of SuHx-treated rats was determined by morphometric analysis of pulmonary vessels following Elastica van Giesson staining. n = 9-14 rats per group. Scale bar: 20 µm. **(E)** Immunofluorescent staining for Ki67 (green) was performed in small pulmonary arteries from vehicle and 6-MP treated rats. SM-actin (red) and nuclei (DAPI) were co-stained with Ki67. The images are representative of n = 9-14 lungs per group. **(F)** Mean cardiomyocyte cross-sectional area (CSA) was assessed in the RV from vehicle and 6-MP treated rats. Scale bar: 20 µm. Quantification of CSA is shown in the bar graph next to the images. n = 9-14 rats per group. **(G)** Picrosirius red staining was performed to assess the fibrosis in the RV from control and 6-MP treated rats. Scale bar: 80 µm. Quantification of fibrosis is shown in the bar graph next to the images. n = 9-14 rats per group. *p<0.05. Student's t-tests were used for comparisons between two groups. Multiple comparisons were assessed by one-way ANOVA, followed by Bonferroni post-hoc test. Error bars, mean ± s.e.m.

Figure 6

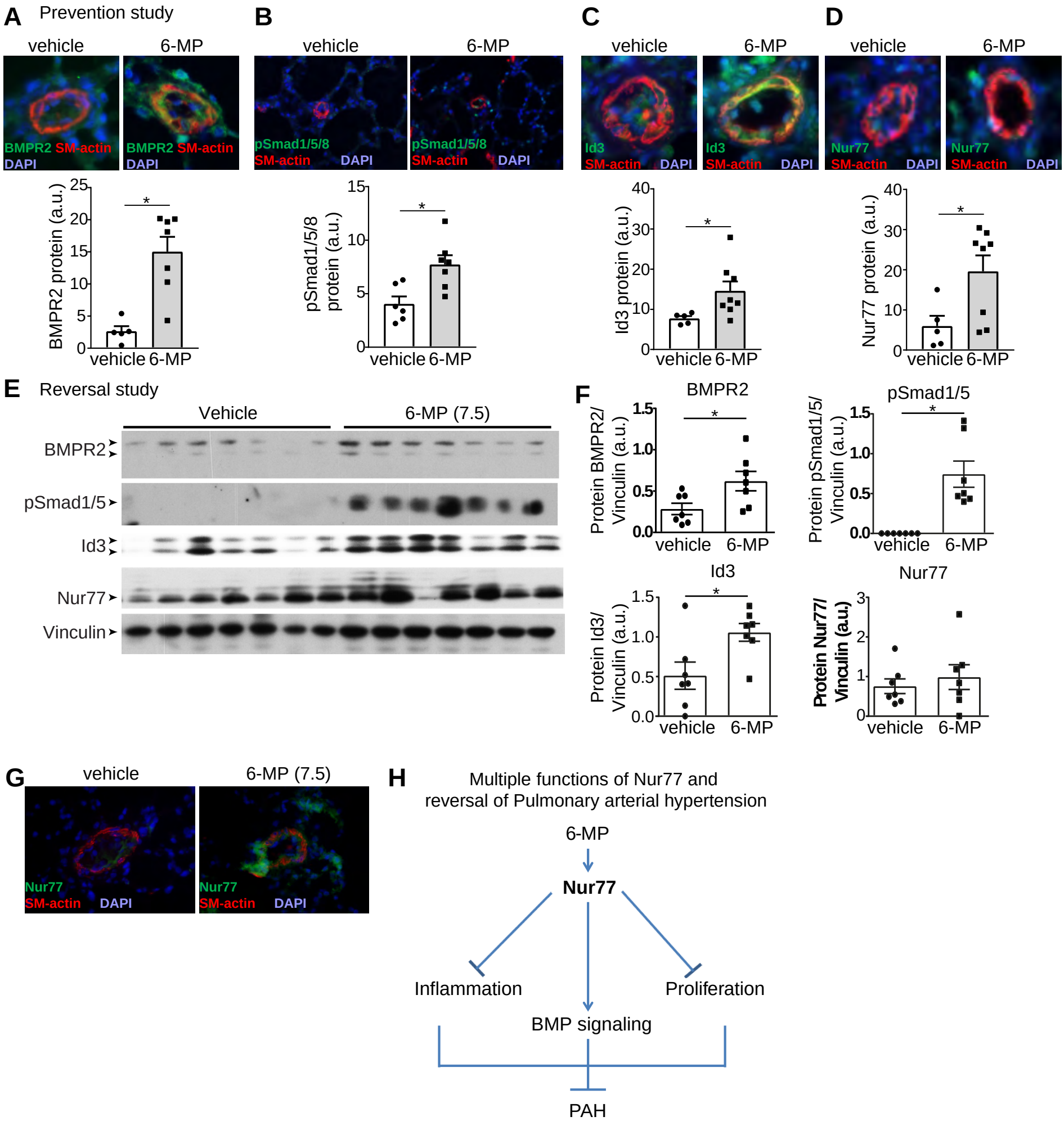

Figure 6: 6-MP enhances Nur77 expression and amplifies BMP signalling in vivo. (A-D) Immunofluorescent staining for BMPR2 (green) (A), pSmad1/5/8 (green) (B), Id3 (green) (C), and Nur77 (green) (D) was performed in small pulmonary arteries from vehicle and 6-MP treated rats from the prevention study. SM-actin (red) defines SMCs and DAPI was used to counterstain nuclei (blue). n = 6-8 lungs per group. **(E)** Western blots showing BMPR2, pSmad1/5, Id3 and Nur77 with vinculin as a loading control in total lung lysates from the SuHx treated rats with vehicle and 6-MP (7.5 mg/kg/day). n = 7 lungs per group. **(F)** Relative densitometric analyses of the western blots showing BMPR2, pSmad1/5, Id3 and Nur77. n = 7 lungs per group. **(G)** Immunofluorescent staining for Nur77 (green) was performed in small pulmonary arteries from vehicle and 6-MP (7.5 mg/kg/day) treated rats. SM-actin (red) and nuclei (DAPI) were co-stained with Nur77. n = 8 lungs per group. *p<0.05. Student's t-tests were used for comparisons between two groups. Multiple comparisons were assessed by one-way ANOVA, followed by Bonferroni post-hoc test. Error bars, mean ± s.e.m. **(H)** Proposed mechanism of Nur77 6-MP in the reversal of PAH. 6-MP increases the transcriptional activity of Nur77 which i) inhibits inflammation through blocking the NFκB pathway; ii) blocks proliferation through inhibition of cell cycle proteins; iii) enhances BMP signalling via activation of the BMPR2-pSmad1/5/8-Id1/3 axis by enhancing BMPR2 expression. Abnormal proliferation and excessive inflammation with impaired BMP signalling leads to initiation and progression of PAH. Activation of Nur77 via clinically approved small-molecule activators such as Nur77 agonist 6-MP reverses these aberrant changes and attenuates PAH.

6-mercaptopurine, an agonist of Nur77, reduces progression of pulmonary hypertension by enhancing BMP signalling

Kondababu Kurakula[1,7], Xiao-Qing Sun[2,7], Chris Happé[2], Denielli da Silva Goncalves Bos[2], Robert Szulcek[2], Ingrid Schalij[2], Karien C. Wiesmeijer[1], Kirsten Lodder[1], Ly Tu[3,4], Christophe Guignabert[3,4], Carlie J.M. de Vries[5], Frances S. de Man[2], Anton Vonk Noordegraaf[2], Peter ten Dijke[6], Marie-José Goumans[1,8], Harm Jan Bogaard[2,8]

[1]Department of Cell and Chemical Biology, Leiden University Medical Center, Leiden, The Netherlands. [2]Pulmonary Hypertension Knowledge Center, Department of Pulmonology, VU University Medical Center/Institute for Cardiovascular Research, Amsterdam, The Netherlands.

[3]INSERM UMR_S 999, LabEx LERMIT, Hôpital Marie Lannelongue, Le Plessis-Robinson, France. [4]Université Paris-Sud et Université Paris-Saclay, Le Kremlin-Bicêtre, France. [5]Department of Medical Biochemistry, Academic Medical Center, Amsterdam, The Netherlands. [6]Department of Cell and Chemical Biology, Oncode institute, Leiden University Medical Center, Leiden, The Netherlands. [7]These two authors contributed equally to this work.[8]These two authors jointly supervised this work.

Supplemental methods:

Human lung samples and cell culture

Control lung tissues and pulmonary arteries were obtained from patients undergoing surgery for lung carcinoma (control). Samples were obtained distant from the malignant lesion and were dissected by a pathologist. Lung tissues and pulmonary arteries were also obtained from iPAH and HPAH-patients undergoing lung transplantation. Lung sample collection was approved by the local ethics committees and written informed consent was obtained. Isolation and culturing of human pulmonary microvascular endothelial cells (MVECs) from lungs of control and PAH patients was described previously [1]. PA-SMCs were isolated and cultured from control donors and described elsewhere [2]. Briefly, SMCs were isolated using the explant technique and used at passage 6 to 8 and were characterized by SM α-actin expression showing uniform fibrillar staining. MVECs from 6 control subjects, 6 iPAH subjects, and 6 HPAH subjects were studied. HEK293T cells were cultured in Dulbecco's modified Eagle's medium (DMEM) with 20 mM glucose, supplemented with 10% serum and penicillin-streptomycin (Invitrogen).

Plasmids and chemicals

Nur77 over-expression plasmids, luciferase reporter constructs: BMP response element (BRE)-luc, CyclinD1-luc, NurRE-luc and NFκB-luc have been described before [3-6]. TNFα and BMP9 were purchased from Peprotech and R&D systems, respectively.

Western blot

Cell lysates were prepared with NP-40 lysis buffer and western blotting was performed as described before [6]. Briefly, cell lysates were resolved by SDS-PAGE, and transferred to polyvinylidene difluoride (PVDF) membranes (Millipore). Blots were blocked with 5% nonfat milk in PBS with 0.1% Tween 20 (PBST) and then developed with diluted antibodies for pSmad1 (1:1000 dilution; pS1 antibody [7]), Nur77 (1:1000 dilution; Abcam), and vinculin (1:1000 dilution; H300; Santa Cruz) at 4°C overnight, followed by horseradish peroxidase-conjugated anti-mouse or anti-rabbit (GE Healthcare) secondary antibodies using an ECL system (Fisher Scientific). Lung tissue of the rats was homogenized in radioimmunoprecipitation assay (RIPA) buffer containing phosphatase and protease inhibitors (Sigma-Aldrich). The protein concentration was quantified by the Pierce 660 nm

protein assay kit (Thermo Scientific). 20 µg protein was used to detect the expression of BMPR2 (1:1000; MA5-15827, Thermo Fisher), phospho-smad1/5/8 (1:1000; 13820, cell signaling) and Id1 (1:500; sc-488, Santa Cruz), and vinculin as loading control (1:1000 dilution; H300; Santa Cruz) at 4°C overnight, followed by appropriate secondary antibody incubation.

Transient transfection and luciferase assays

HEK293T cells were transiently transfected with indicated luciferase reporter plasmids and Nur77 using PEI transfection reagent (Polysciences), following the recommendations of the manufacturer. Primary MVECs were transfected using TransfeX reagent (ATCC) as per the instructions of the manufacturer. β-galactosidase plasmid was co-transfected as an internal control. 48 hours after transfection, the cells were harvested and lysed for measuring the luciferase activity using luciferase reporter assay system from Promega by a Perkin Elmer luminometer Victor3 1420. The amount of plasmid DNA in each well was equalized with an empty vector when necessary and each experiment (in duplicate) was repeated at least three times.

Quantitative Real Time-PCR (qRT-PCR)

Total RNA extraction was performed using NucleoSpin RNA II (Machery Nagel, Düren). cDNA synthesis was performed with iScript (Bio-Rad), followed by real-time PCR using the SYBR Green (Bio-Rad) and a Bio-Rad CFX Connect device. Primers used for real-time PCR are detailed in supplementary table 1. GAPDH served as a control for the amount of cDNA present in each sample. Data were analyzed using the comparative difference in cycle number (ΔCT) method according to the manufacturer's instructions.

Lenti-viral transduction

Recombinant lentiviral particles of overexpression of Nur77 and short hairpin RNAs (shRNAs) targeting Nur77 were produced, concentrated, and titrated as described previously [4]. Five different human shRNAs that target different regions in the Nur77 mRNA were tested and two shRNAs were chosen for generation of lentiviruses based on the efficiency of the knockdown. Lentiviral infection in cultured MVECs was performed as described previously [4]. Transduction efficiency was determined by immunofluorescence, qRT-PCR and western blot.

Cell viability and proliferation assays

3-(4,5-dimethyl-2-thiazolyl)-2,5-diphenyl-2H-tetrazolium bromide (MTT) assays were performed as described previously [3]. Briefly, cells were seeded in a 96-well plate at a density of 3×10^3 cells/well and incubated overnight. Cells were made quiescent by incubation in medium without FCS for 6 h and then incubated overnight with FCS (10% [vol/vol]) for 24 h. After the incubation, cells were incubated with 10 µl of MTT reagent (5 mg/ml) for 3 h at 37°C. 100 µl of isopropanol was added to each well and incubated for 15 min. Colorimetric analysis was performed with an enzyme-linked immunosorbent assay (ELISA) plate reader. Cells were also counted using an automated cell counter (Biorad). Each experiment (in quadruplicate) was repeated at least three times.

SuHx rat model of pulmonary hypertension (PH)

Male Sprague-Dawley rats (bodymass ≈150-220 gr; Charles River) were used throughout the experiment. Rats were housed in standard conditions and food and water was available *ad libitum*. SU5416+Hypoxia (SuHx)-mediated PH was induced according to previously published protocols [8, 9]. Briefly, rats were subjected to a single injection of SU5416 (25 mg/kg, Tocris Bioscience) followed by a 4-week transient exposure to 10% hypoxia and 2 week normoxic re-exposure. In the prevention study, rats received 6-MP (1 mg/kg/day) in drinking water from day 0 to day 42. In the reversal study, after randomization (treatment vs vehicle), animals were divided into two groups receiving 6-MP (1 mg/kg/day or 7.5 mg/kg/day, Sigma–Aldrich) or vehicle (DMSO) in the drinking water from day 42 to day 70. Echocardiography was performed before and after the treatment to study cardiac function. At the end of the experiment (day 42 or day 70) rats were anaesthetized for hemodynamic assessment via RV catheterization, after which rats were exsanguinated. Both lung and cardiac tissues were separated for further analysis. All experiments were approved by an independent local animal ethic committee of the Free university medical center, Amsterdam

(study number VU-FYS 13-01A4), and were carried out in compliance with guidelines issued by the Dutch government.

Echocardiography

All animals underwent echocardiographic assessments (Prosound SSD-4000 and UST-5542) as published previously [9], to measure RV wall thickness (RVWT), RV end diastolic diameter (RVEDD), tricuspid annular plane systolic excursion (TAPSE), stroke volume (SV), heart rate (HR), cardiac output (CO), pulmonary artery acceleration time (PAAT), and cycle length (cl) before and after the treatment, respectively.

Hemodynamic evaluation and RV hypertrophy

Animals were anaesthetized for open-chest RV catheterization (AD Instruments and Millar Instruments) as previously described [8]. RV systolic pressure (RVSP) was determined from steady state measurement, as well as RV afterload (Ea-Arterial elastance). Pressure-volume loops after vena-cava occlusion were obtained and used to derive end-systolic elastance (Ees), and end-diastolic elastance (Eed). Arterial ventricular coupling was calculated as Ees/Ea.

Morphometry of heart and lungs

To assess the extent of RV hypertrophy, the heart was removed and the RV free wall was separated from the left ventricle (LV) and ventricular septum. Wet weights of the RV, free LV and septum were determined separately, and the ratio of RV weight to LV plus septum weight (RV/[LV+S]) was calculated for RV hypertrophy. At the end of experiment, lungs were inflated with an 1% solution of low-melt-agarose and fixed in formalin (overnight) and embedded in paraffin. To determine the pulmonary vascular remodelling, paraffin embedded 5-µm-thick lung sections were stained with Elastica van Giesson to measure the relative wall thickness of pulmonary arterioles (PA), as well as the intimal and medial wall thickness separately, as described previously [8, 9]. The relative wall thickness of PA was calculated as: PA wall thickness = 2* medial wall thickness / outer diameter *100%. For further analysis of RV dimensions, 5-µm-thick sections of frozen cardiac tissues (transversally cut) were stained with haematoxylin and eosin, and a mean cardiomyocyte cross-sectional area (CSA) was assessed. Moreover, picrosirius red staining was used to assess the degree of fibrosis in cardiac cryosections. Level of fibrosis was expressed as the percentage of tissue area positive for collagen compared to total area.

Immunofluorescence microscopy

Human and rat lung tissues were fixed and stained as previously described [10]. Briefly, paraffin sections were deparaffinized and rehydrated. Sections were boiled for 40 min in Vector® Antigen Unmasking Solution (Vector) using a pressure cooker. After blocking with 1% BSA in 0.1% Tween-PBS, sections were incubated overnight at 4°C with primary antibodies directed against Nur77 (1:50; sc-5569, Santa Cruz), Von Willebrand factor (1:1000, Abcam), and alpha smooth muscle actin (1:5000; Sigma). All sections were mounted with ProLong® Gold antifade reagent (Invitrogen) containing DAPI. For the analyses of pulmonary vascular proliferation, 5-µm-thick lung paraffin sections were incubated at 40C overnight with primary Ki67 antibody (1:100; AB9260, EMD Millipore). To determine the pulmonary vascular inflammation, the lung sections were incubated at 40C overnight with primary CD68 (1:1000; ab31630, Abcam), CD20 (1:1000; sc-7735, Santa Cruz) and CD8-antibodies (1:500; ab33786, Abcam) to detect macrophages, B cells and cytotoxic T cells, respectively. Moreover, to analyze the effect of 6-MP on Nur77 and BMP signalling, the following antibodies were used: Nur77 (1:50; sc-5569, Santa Cruz), BMPR2 (1:25; PA5-11863, Thermo Fisher), p-smad1/5/8 (1:2000; 13820, Cell signalling), Cleaved caspase 3 (1:400; 9661; Cell signaling) and Id3 (1:400; sc-490, Santa Cruz). DAPI was used to counterstain the nuclei.

Statistical analysis

Statistical analyses were performed using Graphpad Prism 7 for Windows (GraphPad Software). Student's t-tests were used for comparisons between two groups. Multiple comparisons were assessed by one-way ANOVA, followed by Bonferroni post-hoc test. p-values < 0.05 were considered significant. All statistical tests used two-sided tests of significance. Data are presented as mean ± SEM.

References

1. Szulcek R, Happe CM, Rol N, Fontijn RD, Dickhoff C, Hartemink KJ, Grunberg K, Tu L, Timens W, Nossent GD, Paul MA, Leyen TA, Horrevoets AJ, de Man FS, Guignabert C, Yu PB, Vonk-Noordegraaf A, van Nieuw Amerongen GP, Bogaard HJ. Delayed Microvascular Shear Adaptation in Pulmonary Arterial Hypertension. Role of Platelet Endothelial Cell Adhesion Molecule-1 Cleavage. *American journal of respiratory and critical care medicine* 2016: 193(12): 1410-1420.
2. Long L, Ormiston ML, Yang X, Southwood M, Graf S, Machado RD, Mueller M, Kinzel B, Yung LM, Wilkinson JM, Moore SD, Drake KM, Aldred MA, Yu PB, Upton PD, Morrell NW. Selective enhancement of endothelial BMPR-II with BMP9 reverses pulmonary arterial hypertension. *Nature medicine* 2015: 21(7): 777-785.
3. Kurakula K, Hamers AA, van Loenen P, de Vries CJ. 6-Mercaptopurine reduces cytokine and Muc5ac expression involving inhibition of NFkappaB activation in airway epithelial cells. *Respiratory research* 2015: 16: 73.
4. Kurakula K, van der Wal E, Geerts D, van Tiel CM, de Vries CJ. FHL2 protein is a novel co-repressor of nuclear receptor Nur77. *The Journal of biological chemistry* 2011: 286(52): 44336-44343.
5. Korchynskyi O, ten Dijke P. Identification and functional characterization of distinct critically important bone morphogenetic protein-specific response elements in the Id1 promoter. *The Journal of biological chemistry* 2002: 277(7): 4883-4891.
6. Kurakula K, Vos M, Otermin Rubio I, Marinkovic G, Buettner R, Heukamp LC, Stap J, de Waard V, van Tiel CM, de Vries CJ. The LIM-only protein FHL2 reduces vascular lesion formation involving inhibition of proliferation and migration of smooth muscle cells. *PloS one* 2014: 9(4): e94931.
7. Persson U, Izumi H, Souchelnytskyi S, Itoh S, Grimsby S, Engstrom U, Heldin CH, Funa K, ten Dijke P. The L45 loop in type I receptors for TGF-beta family members is a critical determinant in specifying Smad isoform activation. *FEBS letters* 1998: 434(1-2): 83-87.
8. da Silva Goncalves Bos D, Van Der Bruggen CE, Kurakula K, Sun XQ, Casali KR, Casali AG, Rol N, Szulcek R, Dos Remedios C, Guignabert C, Tu L, Dorfmuller P, Humbert M, Wijnker PJM, Kuster DWD, van der Velden J, Goumans MJ, Bogaard HJ, Vonk-Noordegraaf A, de Man FS, Handoko ML. Contribution of Impaired Parasympathetic Activity to Right Ventricular Dysfunction and Pulmonary Vascular Remodeling in Pulmonary Arterial Hypertension. *Circulation* 2017.
9. de Raaf MA, Kroeze Y, Middelman A, de Man FS, de Jong H, Vonk-Noordegraaf A, de Korte C, Voelkel NF, Homberg J, Bogaard HJ. Serotonin transporter is not required for the development of severe pulmonary hypertension in the Sugen hypoxia rat model. *Am J Physiol Lung Cell Mol Physiol* 2015: 309(10): L1164-1173.
10. Duim SN, Kurakula K, Goumans MJ, Kruithof BP. Cardiac endothelial cells express Wilms' tumor-1: Wt1 expression in the developing, adult and infarcted heart. *Journal of molecular and cellular cardiology* 2015: 81: 127-135.

Supplementary Table 1: Human primer sequences for qRT-PCR

Gene	Primers
IL-6	Fw: CCCACACAGACAGCCACTCA
	Rv: CCGTCGAGGATGTACCGAAT
RANTES	Fw: CGCTGTCATCCTCATTGCTA
	Rv: TGTACTCCCGAACCCATTTC
TNF-α	Fw: AGGACACCATGAGCACTGAAAG
	Rv: AGGAGAGGCTGAGGAACAAG
IL-1β	Fw: TGGCAGAAAGGGAACAGAAAGG
	Rv: GTGAGTAGGAGAGGTGAGAGAGG
Nur77	Fw: GTTCTCGGAGGTCATCCGCAAG
	Rv: GCAGGGACCTTGAGAAGGCCA
BMPR2	Fw: AACTGTTGGSGCTGATTGGC
	Rv: CGGTTTGCAAAGGAAAACAC
Id1	Fw: CTGCTCTACGACATGAACGG
	Rv: GAAGGTCCCTGATGTAGTCGAT
Id3	Fw: CACCTCCAGAACGCAGGTGCTG
	Rv: AGGGCGAAGTTGGGGCCCAT
GAPDH	Fw: AGCCACATCGCTCAGACAC
	Rv: GCCCAATACGACCAAATCC

Figure S1

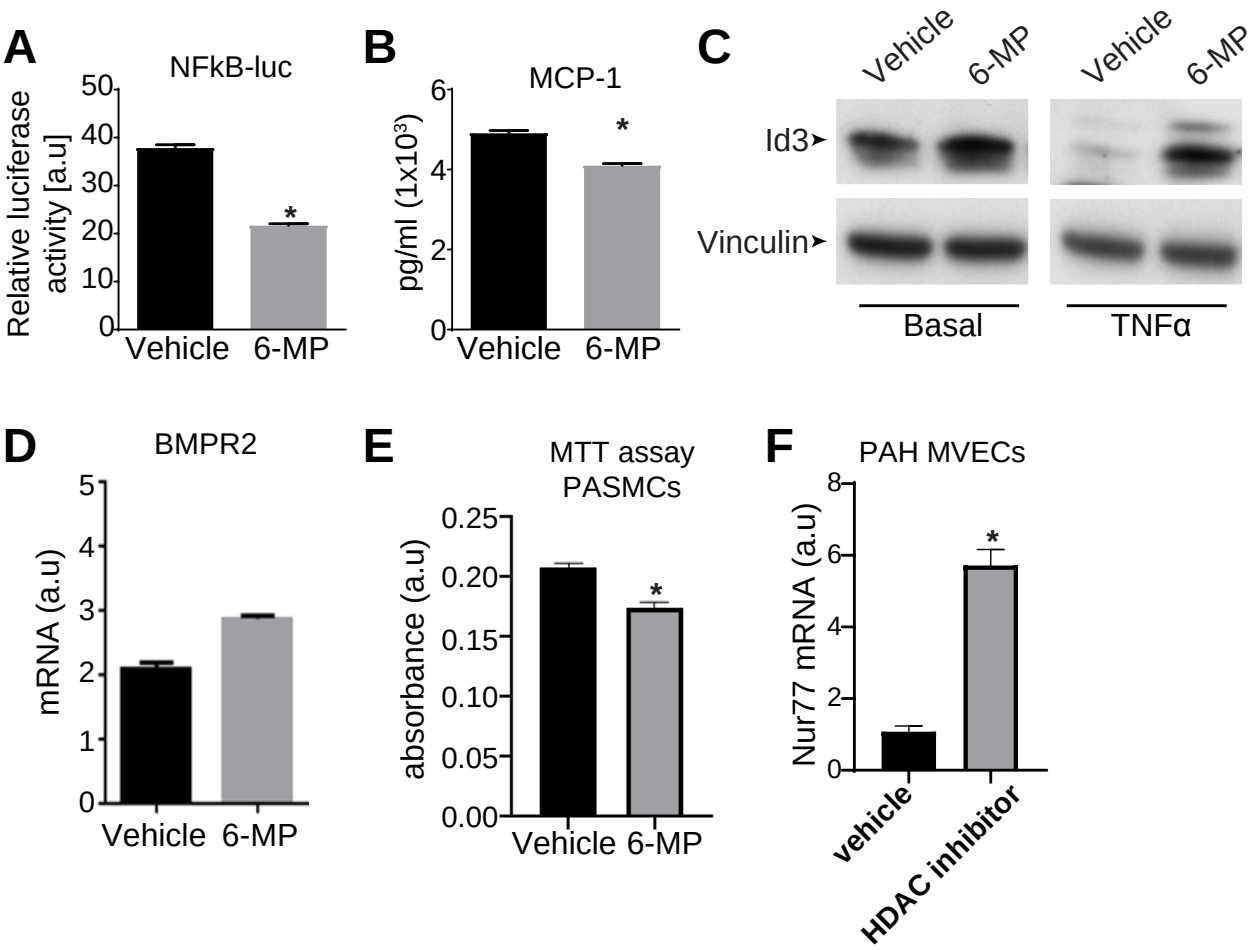

Supplementary Figure 1: 6-MP decreases inflammation and enhances BMP signalling. (A) NFκB-luciferase activity in HEK293T cells was measured following treatment with 6-MP (10 uM) and stimulation with TNFα (50 ng/ml) for 6 h (n=3). **(B)** ELISA for MCP-1 was performed in supernatants from MVECs following treatment with 6-MP (10 uM) and stimulation with TNFα (50 ng/ml) for 6 h (n=3). **(C)** Representative western blots showing Id3 relative to vinculin as loading control under basal and TNFα (50 ng/ml) stimulation and 6-MP (10 uM) treatment for 6 h. **(D)** qRT-PCR was performed to assess mRNA expression of BMPR2 following treatment with 6-MP (10 uM) for 6 h (n=3). **(E)** MTT assays were performed to assess proliferation of healthy human PASMCs following treatment with 6-MP for 24 h (n=3). **(F)** HDAC inhibition significantly increased mRNA levels of Nur77 after treatment of PAH MVECs with the HDAC inhibitor Quisinostat (5uM for 16 h) (n=3). *p<0.05. Student's t-tests were used for comparisons between two groups. Error bars, mean ± s.e.m.

Figure S2

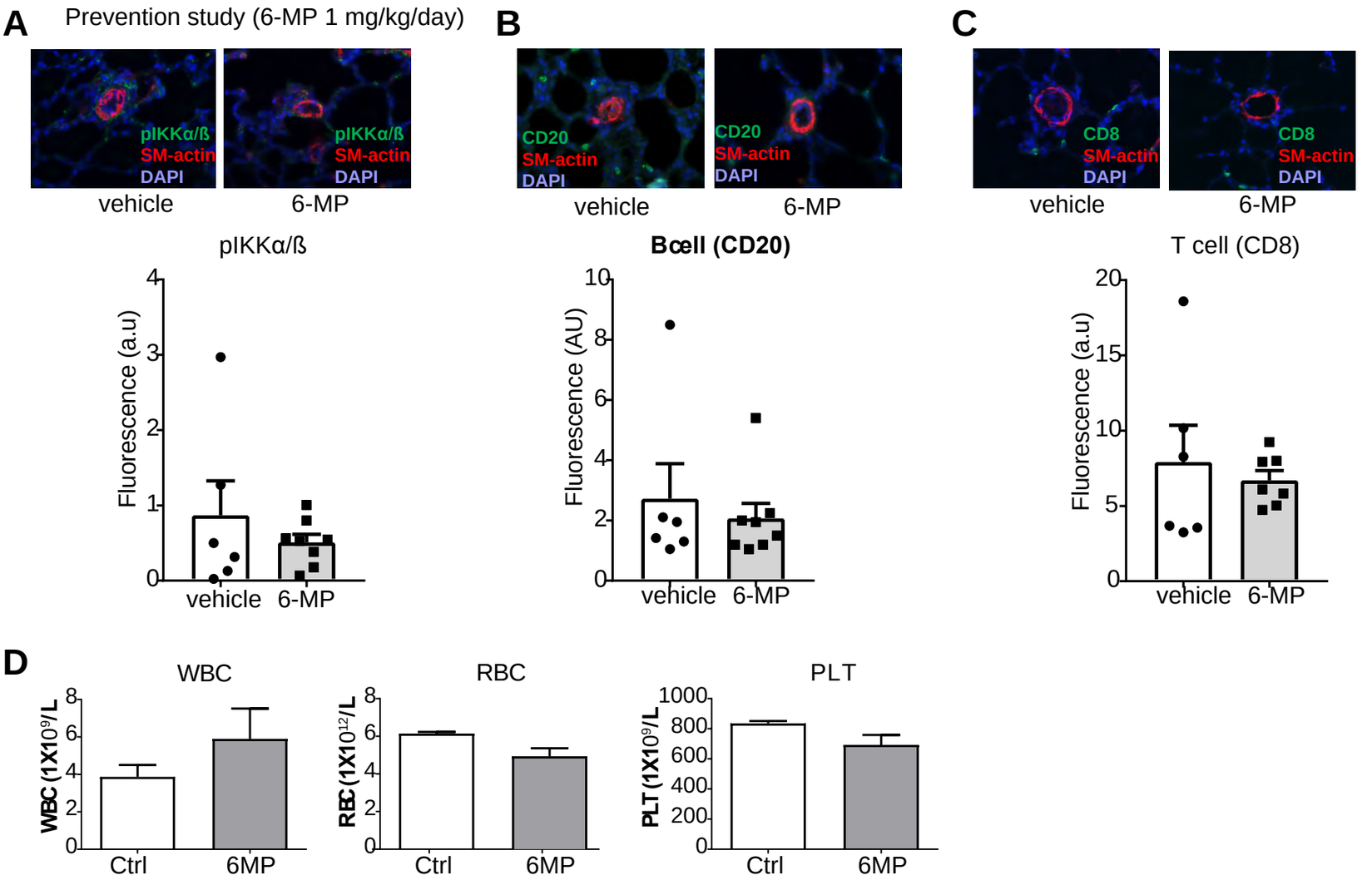

Supplementary Figure 3: 6-MP prevents inflammation and does not change blood cell composition in the prevention study. A-C) Immunofluorescent staining for pIKKα/β (green) (A), CD20 (green) (B) and CD8 (green) (C) in small pulmonary arteries from vehicle and 6-MP treated rats. SM-actin (red) and nuclei (DAPI) were co-stained with pIKKα/β, or CD20 or CD8. Quantification of the fluorescence is shown next to the images. The images are representative of n = 6-8 lungs per group. D) White-blood cells, red-blood cells and platelets were counted using coulter counter after terminating the rats in the prevention study. *p<0.05. Student's t-tests were used for comparisons between two groups. Error bars, mean ± s.e.m.

Figure S3

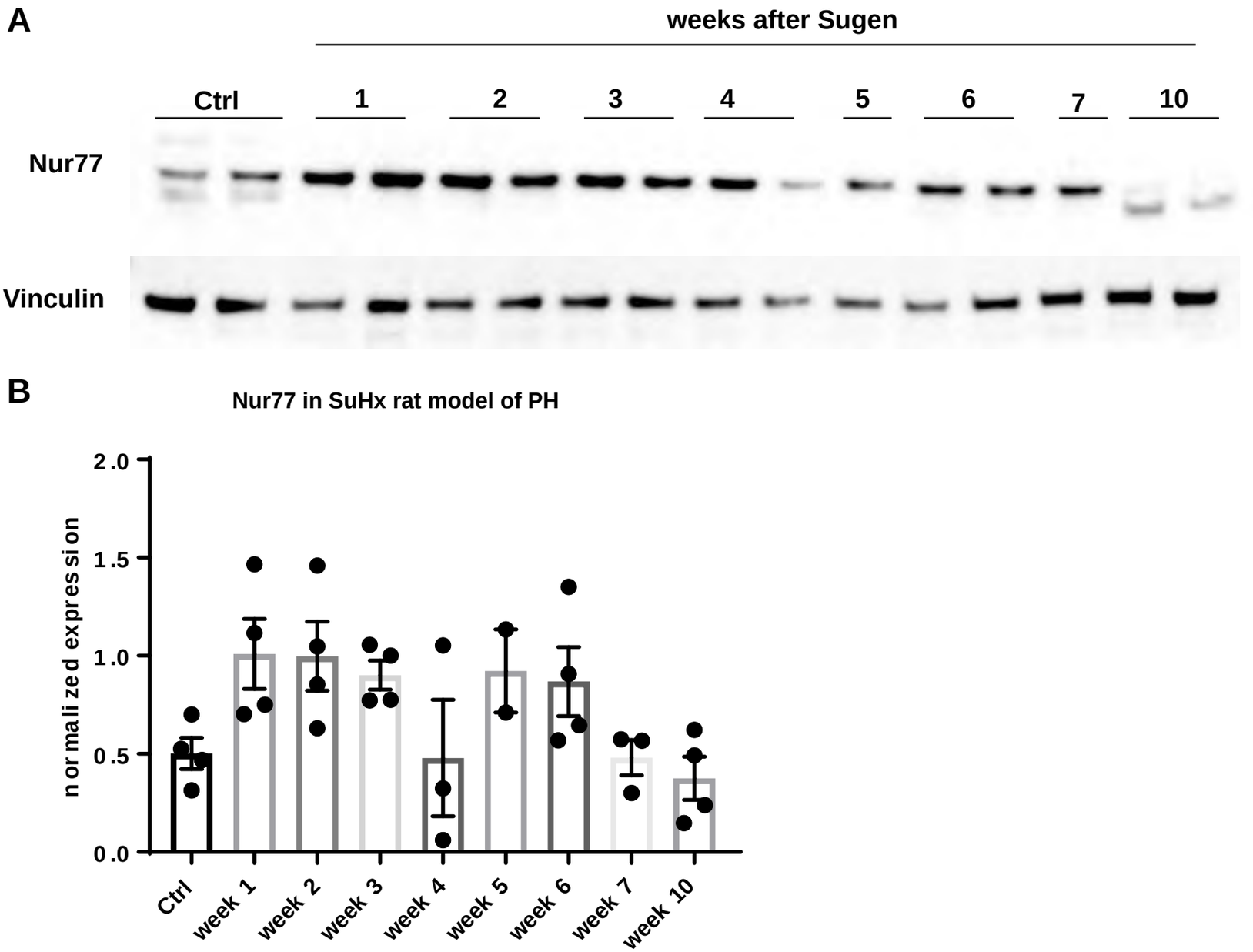

Supplementary Figure 2: Nur77 expression levels during disease progression in SuHx rat model of PH. A-B) Representative western blot (A) and relative densitometric analyses of western blot (B) of Nur77 lung tissue from the SuHx rat model at different time points. Vinculin served as a loading control and used for normalization.

Figure S4

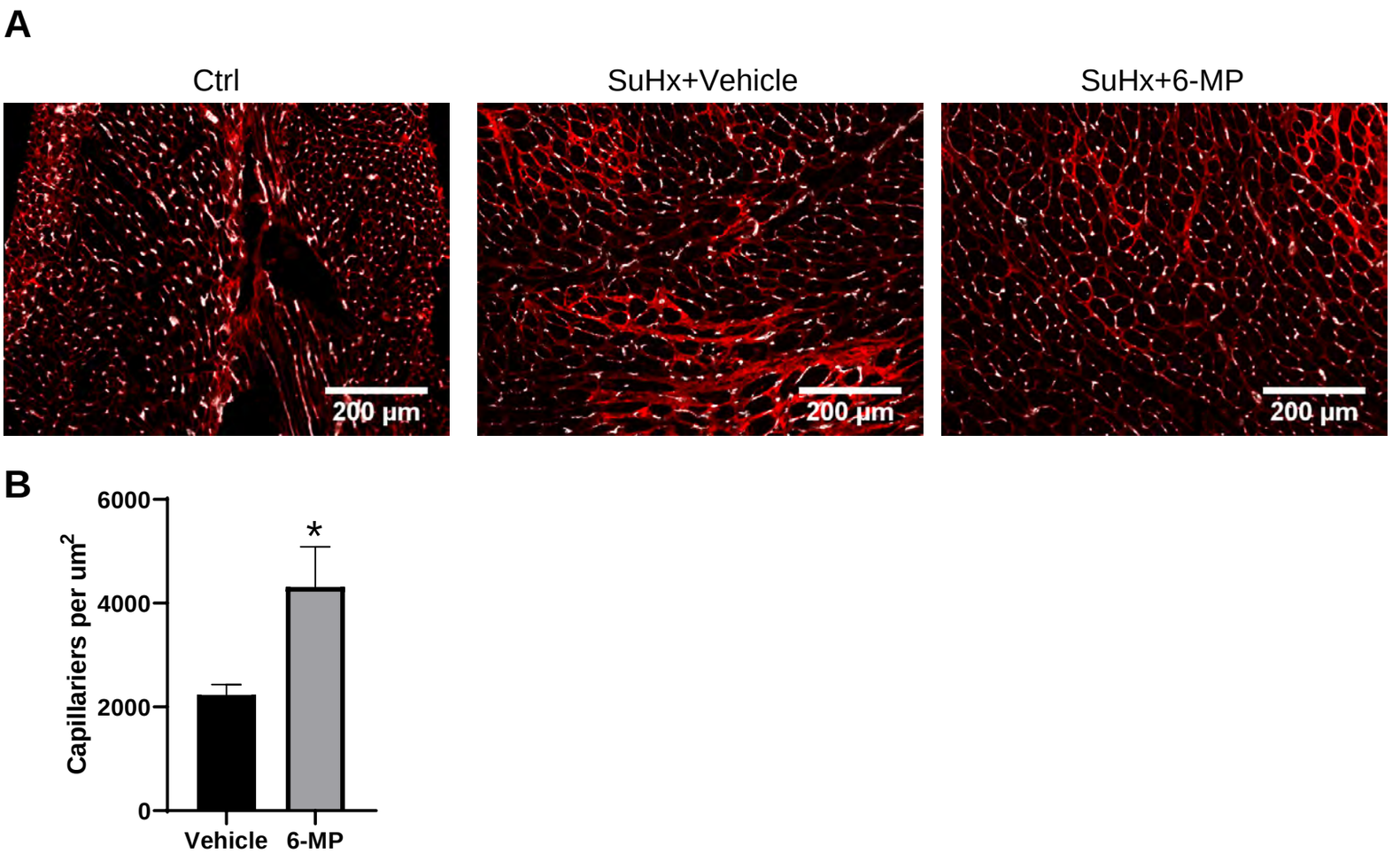

Supplementary Figure 4: 6-MP enhances RV capillary density in SuHx model of PH in the reversal study. (A) Representative immunofluorescence photomicrographs of PECAM-1 (white) and Wheat Germ Agglutinin (WGA, red) in the RV of control, SuHx and 6-MP treated animals (reversal study; n=5-6 per group). **(B)** Number of PECAM-1 positive capillaries were quantified using Image J software.

Figure S5

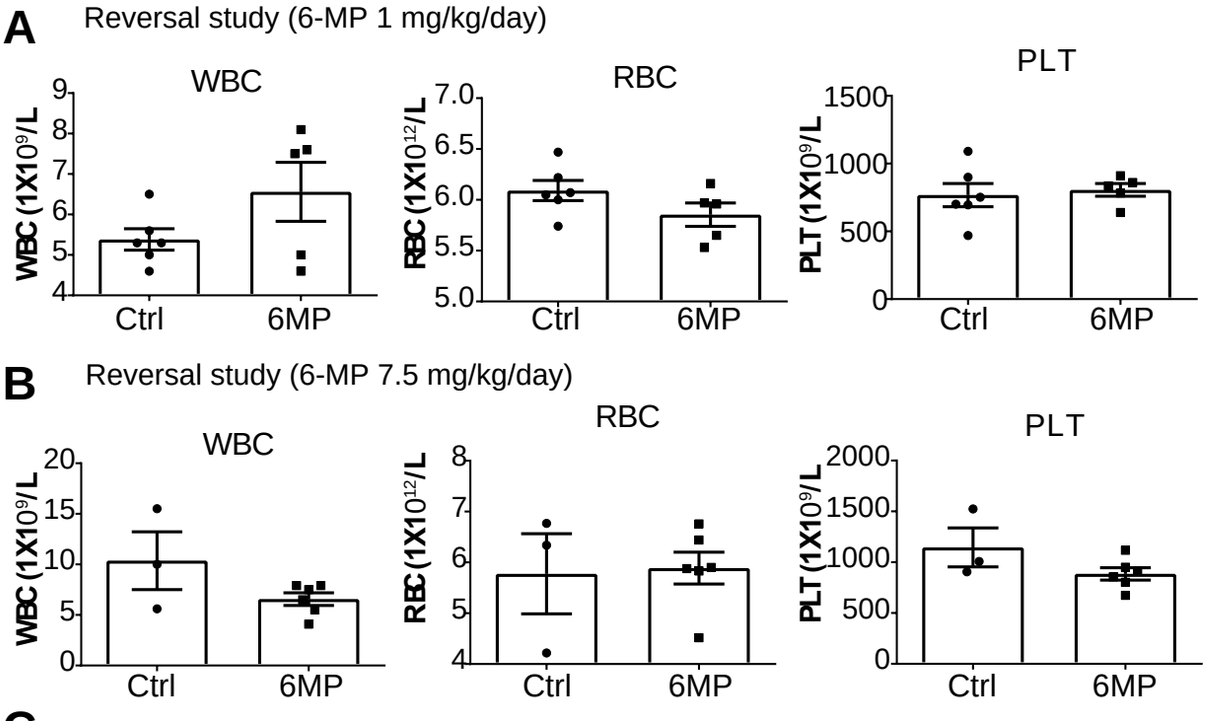

C

	Vehicle	6-MP (7.5)	SD	P-value
Bodyweight week 0	174,6	192,4	21,5	0,139
Bodyweight week 6	447,8	415,9	22,0	0,150
Bodyweight week 10	496,2	475,0	20,3	0,332
Haematocrit (%)	43,2	40,1	2,9	0,513
Heart/tibia length	56,5	49,9	9,2	0,213
Right kidney/tibia length	38,5	37,6	2,7	0,591
Left kidney/tibia length	36,8	37,0	2,5	0,904
Liver/tibia length	457,9	441,9	74,1	0,719
Lungs/tibia length	50,6	52,9	5,0	0,521

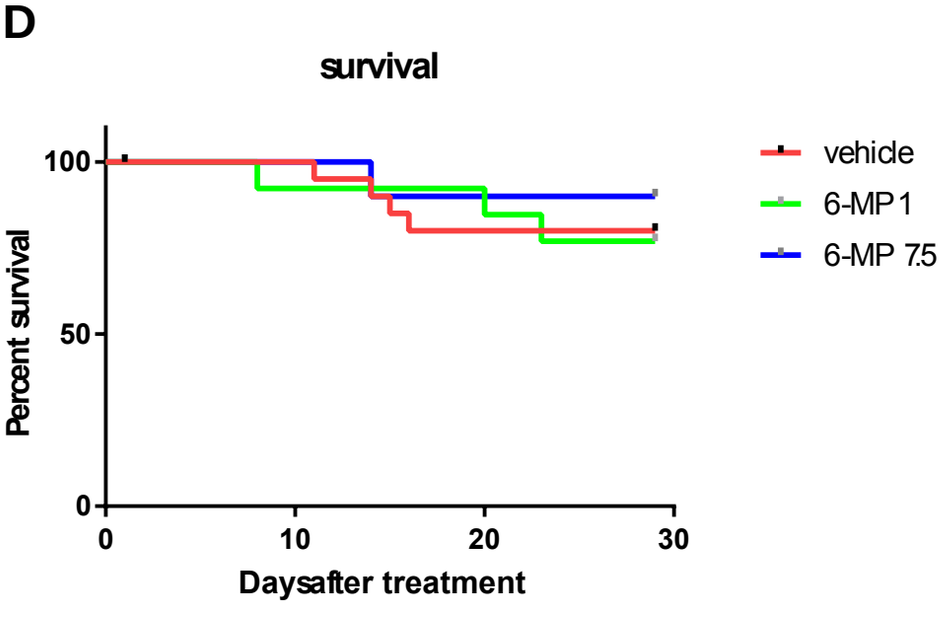

Supplementary Figure 5: 6-MP does not effect on blood cell composition, and improves survival in the reversal study in vivo. A-B) White-blood cells, red-blood cells and platelets were counted using coulter counter after terminating the rats in both the 6-MP 1 mg/kg/day (A) and 7.5 mg/kg/day (B) reversal study. **C)** Autopsy data from the 6-MP 7.5 mg/kg/day reversal study. **D)** Therapeutic dose of 6-MP (7.5 mg/kg/day) improved the survival of experimentally induced PH rats. *p<0.05. Student's t-tests were used for comparisons between two groups. Multiple comparisons were assessed by one-way ANOVA, followed by Bonferroni post-hoc test. Error bars, mean ± s.e.m.

Figure S6

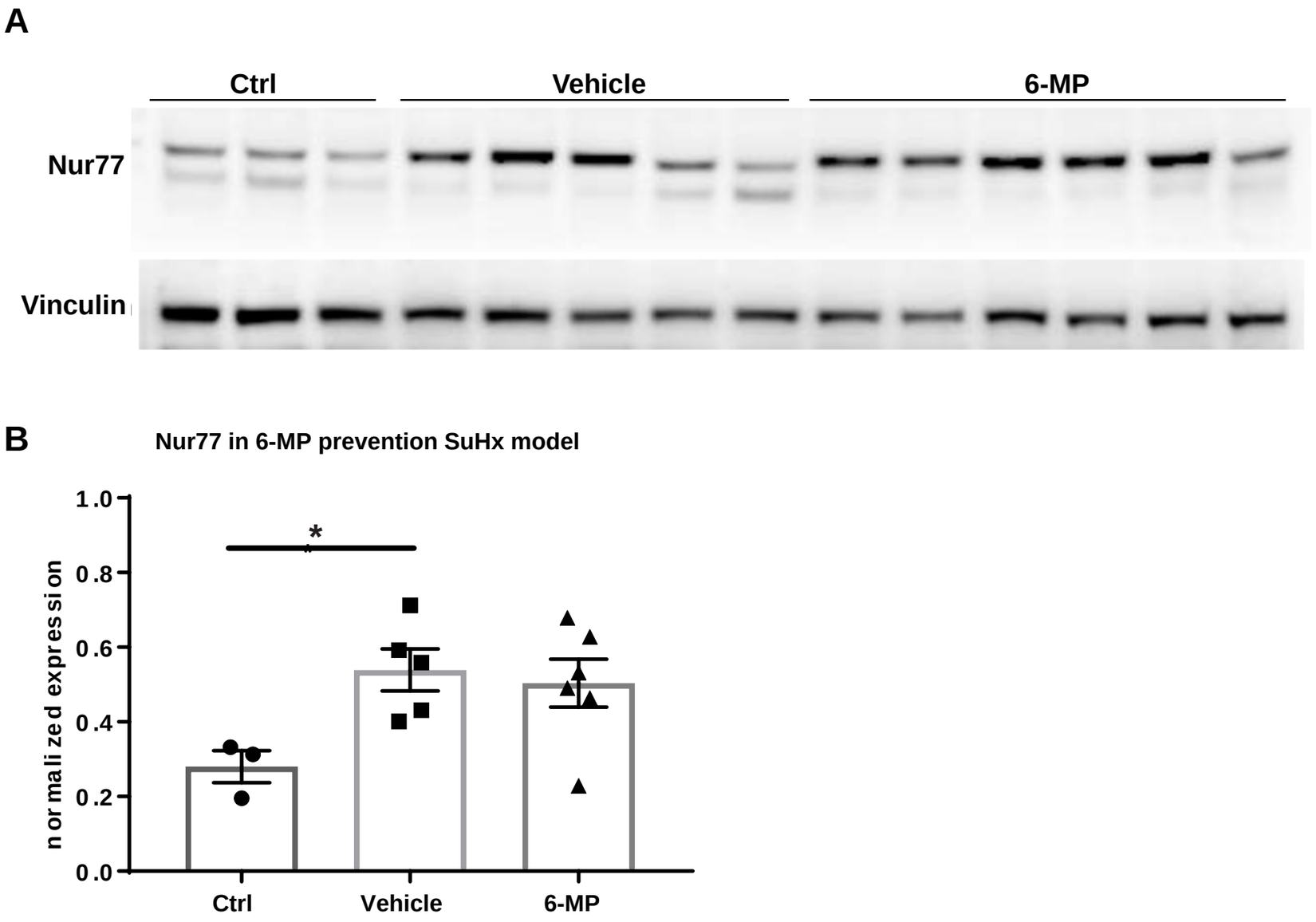

Supplementary Figure 6: The expression levels of Nur77 in the SuHx rat model of angioproliferative PH. A-B) Representative western blot (A) and relative densitometric analyses of western blot (B) of Nur77 in total lung lysates form control, vehicle and 6-MP prevention study was performed (time point 6 weeks). Vinculin served as a loading control and used for normalization.

Figure S7

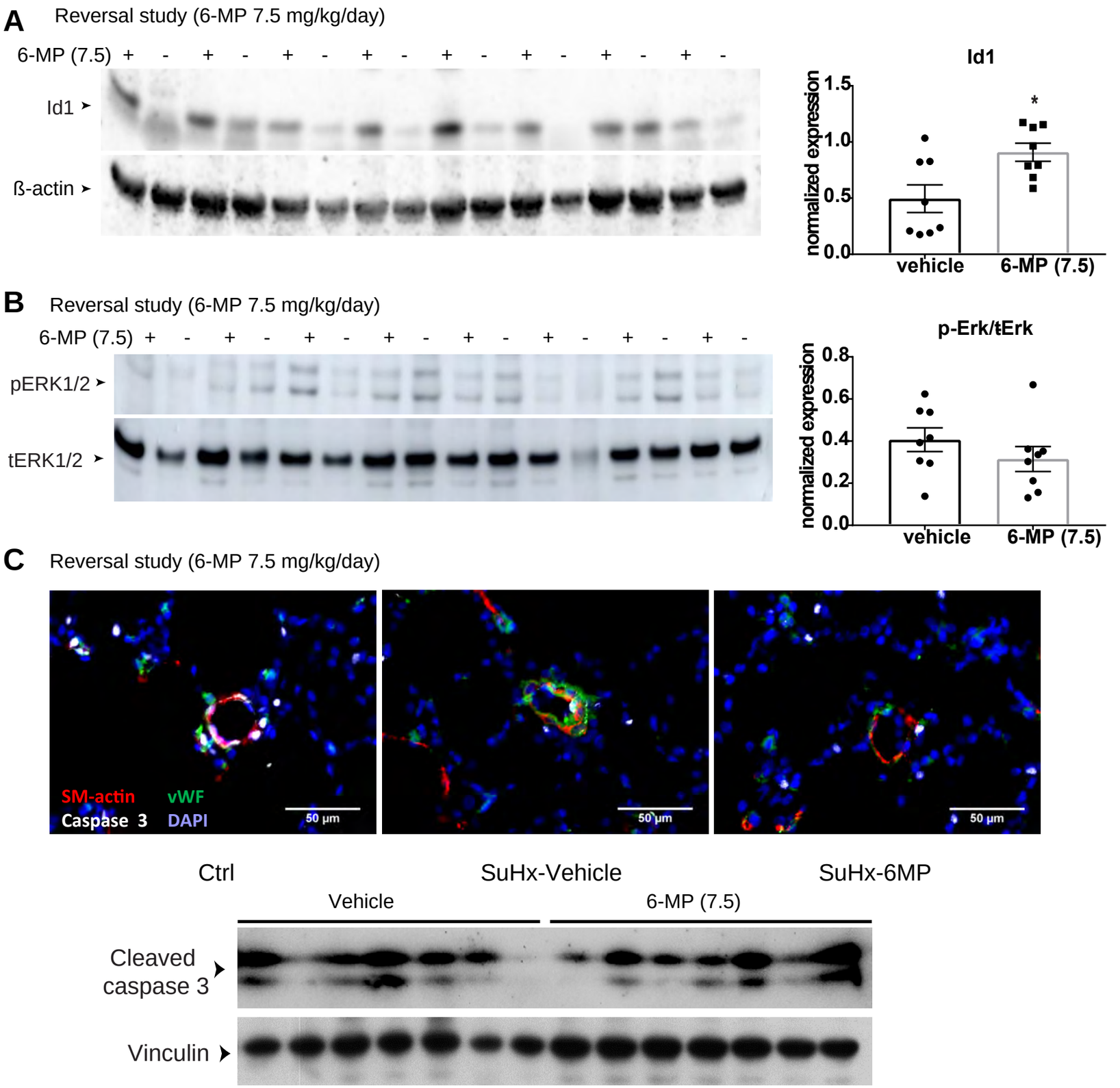

Supplementary Figure 7: 6-MP enhances Id1 expression, but has no significant effect on pERK1/2 and caspase activation. **A-B)** Western blots of lung lysates from therapeutic dose of 6-MP reversal study. Relative densitometric analyses showing Id1 **(A)** and pERK1/2 **(B)** relative to β-actin and total ERK1/2, respectively (n=8). *p<0.05. Multiple comparisons were assessed by one-way ANOVA, followed by Bonferroni post-hoc test. Error bars, mean ± s.e.m. **(C)** Representative immunofluorescence photomicrographs of Caspase 3 (white), α-smooth muscle actin (SM-actin, red), and Von Willebrand factor (vWF, green) in the lungs from 6-MP reversal study. DAPI (blue) (upper panel). Western blots of lung lysates from therapeutic dose of 6-MP reversal study for cleaved caspase 3 (lower panel).